REMODELING OF THE HDL PHOSPHOLIPIDOME BY ABCG1 CONTRIBUTES TO ITS ATHEROPROTECTIVE PROPERTIES

Lise M. Hardy[1], Marie Lhomme[2], Lucie Poupel[1], Isabelle Guillas[1], Maharajah Ponnaiah[2], Eric Frisdal[1], Maryline Olivier[1], Petra El Khoury[1*], Elise F. Villard[1], Jean-François Franetich[3], Hervé Durand[1], Yuri V. Bobryshev[1], Philippe Lesnik[1], Emmanuel L. Gautier[1], Thierry Huby[1], Wendy Jessup[4], Alain Carrié[1,5], Eric Bruckert[1,5], Maryse Guerin[1], Anatol Kontush[1] and Wilfried Le Goff[1].

Affiliations

[1]Sorbonne Université, Inserm, Institute of Cardiometabolism and Nutrition (ICAN), UMR_S1166, Hôpital de la Pitié, Paris, F-75013, France

[2]ICANalytics lipidomic, Institute of Cardiometabolism and Nutrition (ICAN), Paris, France

[3]Sorbonne Université, Inserm, Centre d'Immunologie et des Maladies Infectieuses (CIMI), UMRS_1135, Hôpital de la Pitié, Paris, F-75013, France

[4]Atherosclerosis Group, ANZAC Research Institute, University of Sydney, Australia.

[5]AP-HP Assistance Publique-Hôpitaux de Paris, Pitié-Salpêtrière, Paris, France

*Current address : Laboratory of Biochemistry and Molecular Therapeutics, Faculty of Pharmacy, Pôle Technologie- Santé, Saint Joseph University, Beirut, Lebanon; INSERM LVTS U1148, Hôpital Bichat-Claude Bernard, Paris, France.

Corresponding author

Wilfried Le Goff, PhD.

INSERM UMR_S1166

Faculté de médecine Sorbonne Université

91, boulevard de l'Hôpital

75013 Paris

France

Email : wilfried.le_goff@sorbonne-universite.fr

Words : 8345

Subject codes

Lipids and cholesterol, metabolism, Atherosclerosis, Cardiovascular Diseases

Short title

Modulation of HDL phospholipidome by ABCG1

Abstract.

Rationale. Circulating concentrations of cholesterol associated with high-density lipoproteins (HDL) are negatively correlated with atherosclerotic cardiovascular diseases. The capacity of HDL to promote macrophage cholesterol efflux is considered to underlie the atheroprotective function of HDL. Phospholipidome of HDL is a critical determinant of their function, however mechanisms controlling both HDL phospholipidome and function are unknown.

Objective. To determine if the ATP-binding cassette G1 (ABCG1) transporter could modulate atheroprotective functions of HDL through the remodeling of their phospholipidome.

Methods and Results. *In vitro* remodeling of HDL2 by ABCG1 led to an enhancement of its anti-inflammatory property and capacity to promote cholesterol efflux in primary human macrophages. Immunodetection of ABCG1 in human liver biopsies revealed that ABCG1 is highly expressed in hepatocytes and ABCG1 knockdown (KD) in primary human hepatocytes (PHH) significantly decreased cholesterol efflux to HDL (-26%, $p<0.0005$). Transient hepatic expression of human ABCG1 in complementary mouse models induced a modification of the phosphosphingolipidome of HDL and enhanced its capacity to promote human THP-1 macrophage cholesterol efflux (+38%, $p<0.05$). Analysis of a frequent polymorphism of the *ABCG1* gene (rs1378577, T/G) in normolipidemic women confirmed the ABCG1-mediated remodeling of the HDL phosphosphingolipidome together with the impact on human THP-1 macrophage cholesterol efflux (TT>GG, +31%, $p<0.005$). In addition, analysis of the phosphosphingolipidome of human HDL2 following incubation with control or ABCG1 KD PHH indicated that the ABCG1-remodeling of PL in HDL2 mainly occurs at the hepatic level. Finally, the abundance of PE 36:5 in HDL2, which was reduced by ABCG1, was strongly correlated with carotid and femoral intima-media thickness ($r=0.61$, $p=0.03$ and $r=0.82$, $p=0.001$, respectively) in women.

Conclusions. We uncovered a mechanism under the control of ABCG1 that modifies the phospholipidome of HDL and enhances its atheroprotective function. Such an ABCG1-remodeling of HDL might protect from atherosclerosis in women.

Abbreviations.

ABCG1 : ATP-Binding Cassette G1

Apo : Apolipoprotein

ASCVD : Atherosclerotic cardiovascular diseases

CCA : Common carotid artery

Cer : Ceramide

CETP : Cholesteryl ester transfer protein

CFA : Common femoral artery

HDL : High-density lipoproteins

HMDM : Human monocyte-derived macrophages

KC : Kupffer cells

KD : Knockdown

LPC : Lysophosphatidylcholine

LPE : Lysophosphatidylethanolamine

PA : Phosphatidic acid

PC : Phosphatidylcholine

PE : Phosphatidylethanolamine

PG : Phosphatidylglycerol

PHH : Primary human hepatocyte

PI : Phosphatidylinositol

PL : Phospholipid

pPE : plasmalogen PE

PS : Phosphatidylserine

RNAi : RNA interference

SM : Sphingomyelin

TC : Total cholesterol

TG : Triglyceride

Introduction.

Atherosclerotic Cardiovascular Diseases (ASCVD) are the leading cause of morbidity and mortality in Western countries. It is well established that circulating concentrations of cholesterol associated with high-density lipoproteins (HDL-C) are negatively correlated with ASCVD incidence, rending HDL-C a key component for predicting cardiovascular risk[1–3]. Multiple biological activities are displayed by HDL including cellular cholesterol efflux, antioxidative, anti-inflammatory, anti-infectious and vasodilatory activities[4]. Among them, HDL capacity to promote cholesterol efflux from macrophages in the early step of reverse cholesterol transport, a process through which cholesterol returns to the liver for biliary secretion, is proposed to underlie the association between HDL-C and ASCVD. Indeed, the capacity of HDL to promote macrophage cholesterol efflux is inversely associated with atherosclerosis development[5], incident CV events[6] and mortality in patients with myocardial infarction[7] independently of HDL-C levels. Those studies paved the way to the notion that HDL functionality could represent a better indicator of ASCVD risk than HDL-C levels[8].

Structure (size and shape) and composition (lipid and protein content) of HDL particles are highly heterogeneous[4,9], with such a heterogeneity being intimately linked to their biological functions[10]. By contributing up to 30% of total lipid mass, phospholipids (PL) are the predominant lipid class composing HDL particles; we previously reported that the HDL phospholipidome is an important modulator of atheroprotective property of HDL[11,12]. Alterations of both the phospholipidome and biological functions of HDL are detected in ASCVD patients suggesting that the abundance of PL molecular species within HDL is associated with the CVD risk[13–16].

The membrane ATP binding cassette G1 (ABCG1) transporter is able to promote the export of numerous molecules, mostly lipids[17], which include PL[18,19] through the cellular membrane. Although ABCG1-mediated efflux to non-specific acceptors such as albumin may occur, large HDL particles (but not lipid-free apolipoprotein A-I (ApoA-I)) are major lipid acceptors for ABCG1[19,20]. Through this mechanism, ABCG1 was reported to control tissue lipid homeostasis[21,22] but there is still no evidence for a direct role of ABCG1 in HDL function[17]. In familial hypercholesterolemia, ABCG1-mediated cholesterol efflux to large HDL2 was reported to be inversely associated with carotid intima-media thickness[23]. The HDL2

particles are the predominant cholesterol acceptors for cellular cholesterol efflux in normolipidemic women[24] and we previously reported that the genetic variation of *ABCG1* contributes to a higher proportion in the capacity of plasma to promote macrophage cholesterol efflux in women than in men, an effect that is independent of circulating HDL-C concentrations[25].

In the present study, we addressed the hypothesis that ABCG1 could modulate HDL function through the remodeling of their phospholipidome. Using a translational approach, we demonstrated that hepatic human ABCG1 impacts the abundance of specific PL species in HDL particles and enhances their capacity to promote macrophage cholesterol efflux. Moreover, our findings led us to propose that such a compositional rearrangement mediated by ABCG1 might protect against atherosclerosis in women with the identification of PL species underlying this effect.

Methods.

Isolation and characterization of plasma HDL

Human HDL2. Human HDL2 were isolated from human plasma or culture medium by a multistep ultracentrifugation procedure. Briefly, the density of plasma was increased to 1.063 g/ml by addition of dry solid potassium bromide. Apolipoprotein (apo)B-containing lipoproteins (d < 1.063 g/ml) were removed from cell culture medium or plasma after a first ultracentrifugation at 45,000 rpm for 24 h at 15°C using a Beckman 50.4 rotor in a Beckman XL70 ultracentrifuge. The density of the d<1.063 g/ml fraction was adjusted to 1.125 g/ml by addition of dry solid potassium bromide. Then HDL2 lipoproteins (d 1.063- 1.125 g/ml) were obtained following a second ultracentrifugation at 45,000 rpm for 48 h at 15°C using a Beckman 50.4 rotor in a Beckman XL70 ultracentrifuge. Study population was part of the normolipidemic population previously described[25] consisted of women homozygous carriers for either the TT (n=40) or the GG (n=28) genotype of the frequent functional rs1378577 (ABCG1 c. -134 T>G) single nucleotide polymorphism. Major clinical and biochemical characteristic of the study population are presented in the Supplemental Table 1. Carotid and femoral ultrasonography was performed in a subset of individuals (n=12) by high-resolution B-mode ultrasound of the common carotid artery (CCA), the carotid bifurcation, the internal carotid artery, and the common femoral artery (CFA) as previously described[26]. The study was performed in accordance with ethical principles outlined in the declaration of Helsinki. Written informed consent was obtained from all patients.

Mouse HDL. ApoB-containing lipoproteins (d < 1.063 g/ml) were removed from mouse plasma by ultracentrifugation at 120,000 rpm for 3 h at 15°C using a Beckman TLA 120.2 rotor in a Beckman Optima Max TL ultracentrifuge. Then, total HDL (d 1.063–1.21 g/ml) was isolated from ApoB-depleted plasma by ultracentrifugation at 120,000 rpm for 5 h at 15°C using a Beckman TLA 120.2 rotor in a Beckman Optima Max TL.

Purified HDL fractions of human or murine origin were dialyzed using Spectrapor membrane tubing against Phosphate Buffer Saline at pH7.4 before analysis for their lipid and protein content and used in functional assays.

Biochemical analysis. Human HDL2 and mouse HDL lipid and protein levels were analyzed using routine enzymatic methods on an autoanalyzer Konelab 20 (Thermo Scientific, Cergy Pontoise, France). Commercial kits were used for the determination of total cholesterol, phospholipid (Diasys, Grabels, France), triglycerides and protein (Thermo Scientific, Cergy Pontoise, France) concentrations. Human. ApoB-depleted plasma from hApoB/CETP mice was obtained following dextran sulfate-magnesium precipitation of apolipoprotein B-containing lipoproteins (Biomérieux, Craponne, France).

Human ABCG1-mediated remodeling of HDL lipoproteins.

Remodeling of HDL2 by human ABCG1 was achieved by incubating isolated human HDL2 with either control cells or cells in which human ABCG1 expression was stably expressed (CHO-K1 cells[20]) or knocked down by RNAi (Human hepatocytes) in serum-free media for 16h at 37°C. Subsequently, media containing remodeled HDL2 were centrifuged at 1,500 rpm for 5 min in order to discard cell debris and HDL2 were reisolated by ultracentrifugation as described above.

Lipidomic analysis of high-density lipoproteins.

All internal standards were purchased from Avanti Polar Lipids (Alabaster, AL, USA). LC/MS grade or UPLC grade solvents were used without further purification and obtained from Sigma-Aldrich (St Louis, MO, USA).

Human HDL2 and mouse HDL (30µg PL) were extracted using a modified Bligh and Dyer protocol. Briefly samples supplemented with a mixture of internal standards were mixed with 1600 µL of acidified methanol:0.1N HCl (1:1 v/v) and 800 µL chloroform as described elsewhere[11,12]. The lower organic phase was dried, lipids were reconstituted into 40µL of LC/MS compatible solvent and lipids quantified by LC-ESI/MS/MS. Quantification of phospholipids, sphingolipids and neutral lipids was performed in positive-ion mode. Sample was injected to a Kinetex HILIC 2.6µm 2.1x150mm column (Phenomenex, CA, USA). Mobile phases consisted of water and acetonitrile containing ammonium acetate and acetic acid. Lipid species were detected using scheduled multiple reaction monitoring (sMRM) and quantified using thirty-seven calibration curves specific for the 16 individual lipid subclasses and up to 12 fatty acid moieties. More abundant lipid species were quantified from a 10-fold diluted sample. An in-house

developed R script was used to correct for isotopic contribution to MRM signals as adapted from Ejsing CS et al[27].

Human macrophages

Blood monocytes were isolated from healthy normolipidemic donors (Etablissement Français du Sang, EFS) by Ficoll gradients (Ficoll-Paque PLUS, GE Healthcare) and subsequently differentiated into human macrophages by adhesion on plastic Primaria plates (Falcon) over a period of 10 days of culture in RPMI 1640 medium supplemented with 10% heat-inactivated human serum, 2 mmol/L glutamine, 80 U/mL penicillin/streptomycin and 20 ng/mL human macrophage colony-stimulating factor. Inflammation was triggered in HMDM by incubation with 50ng/mL lipopolysaccharides for 8h and cytokine secretion was quantified in the culture media as previously described[28]. Human THP-1 monocytic cells were obtained from the American Type Culture Collection (ATCC) and maintained in RPMI 1640 medium supplemented with 10% heat-inactivated FBS, 2 mmol/L glutamine and 100 U/mL penicillin/streptomycin at 37°C in 5% CO_2. THP-1 were differentiated into macrophage-like cells with 50 ng/mL phorbol 12-myristate 13-acetate for 48h.

Human hepatocytes

Human hepatocytes were isolated from liver fragments obtained from adult patients undergoing partial hepatectomy. All hepatocytes were isolated using collagenase perfusion as previously described[29]. Human primary hepatocytes were cultured in William's Medium E (Life Technologies) supplemented with 10% FCS (Perbio), 5×10^{-5} M hydrocortisone hemisuccinate (Upjohn Laboratories SERB, France), 5 µg/ml insulin (Sigma), 2 mM L-glutamine and 200 U/ml penicillin, 200 µg/ml streptomycin (Life Technologies, Courtaboeuf, France). The human hepatocellular carcinoma cell line Hep3B was obtained from the American Type Culture Collection (ATCC) and grown in Dulbecco's Modified Eagle's Medium supplemented with 10% FBS, 2 mM glutamine, 1% non-essential amino acids and 100 U/mL penicillin/streptomycin at 37°C in 5% CO_2.

Transient expression of human ABCG1 in mice.

Mouse models. *Atp-binding cassette g1 (Abcg1)*$^{-/-}$ mice were generated at the Institut Clinique de la Souris (Strasbourg, France). Abcg1 mutant ES cell clones from C57BL/6 N mice were purchased from

the European Conditional Mouse Mutagenesis Program (EUCOMM). The Abcg1 targeting vector was constructed following the insertion of a gene-trap LacZ cassette downstream the exon 4 of the *Abcg1* gene (Supplemental Figure 1). Human ApoB/human CETP (ApoB/+;CETP/+) double transgenic mice were generated by breeding human CETP transgenic mice (line 5203) with mice transgenic for the human apoB gene as previously described[30].

Experimental procedure. Twelve-week aged female mice fed a standard chow diet were retro-orbitally injected with 40µg of either hABCG1 expression vector[20] or control parent pcDNA4.0 vector using an in vivo transfection reagent (PepJet DNA In Vivo Transfection Reagent, SignaGen Laboratories, injected volume 200µl) under isoflurane anesthesia. Seven days following the injection, blood samples were collected in Microvette tubes (Sarstedt, Marnay, France) by retro-orbital bleeding under isoflurane anesthesia. Mice were weighed, euthanized and their livers were isolated. Plasma samples were analyzed with an Autoanalyzer (Konelab 20) using reagent kits from Roche for TC and ThermoElectron for HDL-C. A liver piece was excised, minced and digested in Hank's balanced salt solution (HBSS, Gibco, Invitrogen, Cergy Pontoise, France) with 2.5 mg/mL collagenase D (Roche, Boulogne Billancourt, France) for 30 min at 37°C under shaking at 125 rpm and dissociated through a 100 µm pored cell strainer (Franklin lakes, NJ, USA). Hepatocytes were isolated following a brief centrifugation for 1 min at 1,000 rpm and stored at -80°C until use.

RNAi-mediated silencing of human ABCG1 expression

ABCG1 knock-down (KD) cells were obtained by transfection of siRNA oligonucleotides (Dharmacon) targeted to the cDNA sequence of the human ABCG1 gene using lipofectamine RNAiMax (Invitrogen) as previously described[31]. After a 24-h incubation at 37°C, ABCG1 KD and control cells were used for subsequent experiments.

RNA extraction, retrotranscription and real-time quantitative PCR

Total RNAs from cell cultures or tissues were extracted using the NucleoSpin RNA II kit (Macherey-Nagel) according to the manufacturer's instructions. Reverse transcription and real-time qPCR using a LightCycler LC480 (Roche) were performed as previously described[31]. Human mRNA levels were normalized to those of human non-POU domain-containing octamer-binding housekeeping gene

(NONO), human alanine (*ALA*), human α-tubulin (*TUBA*) and human heat shock protein 90kDa alpha (cytosolic), class B member 1 (*HSP90AB1*), human hypoxanthine phosphoribosyltransferase 1 (*HPRT1*), and human 18S ribosomal RNA (18S rRNA). Mouse mRNA levels were normalized to those of mouse hypoxanthine phosphoribosyltransferase 1 (*Hprt1*), mouse non-POU domain-containing, octamer-binding housekeeping gene (*Nono*), mouse heat shock protein 90kDa alpha (cytosolic), class B member 1 (*Hsp90ab1*) and mouse cyclophilin A (*CycA*). Data were expressed as a fold change in mRNA expression relative to control values.

Cellular cholesterol efflux

Cells were labelled for 24h in serum-free media supplemented with 0.2% BSA containing either 50µg/mL acetylated LDL (human macrophages) or 10% serum (human hepatocytes) labelled with 1µCi/mL [^{3}H]cholesterol. The labeling medium was removed and the cells were washed twice with PBS and incubated with serum-free media supplemented with 0.2% BSA for additional 16h. Afterwards, cells were washed twice with warm serum-free media supplemented with 0.2% BSA and incubated with either 15 µg/mL HDL-PL (total HDL or HDL2) or 1% plasma for 4h. Radioactivity content was determined in the media and cells following extraction in hexane-isopropanol (3:2) by liquid scintillation counting (Wallac Trilux 1450 Microbeta, Perkin Elmer, Villebon-sur-Yvette, France). The percentage of free cholesterol efflux was calculated as 100 x (medium cpm) / (medium cpm + cell cpm). Cholesterol efflux to exogenous acceptors was determined by subtracting free cholesterol efflux measured in the absence of exogenous acceptors.

Western blotting analysis

Cell proteins were extracted using NE-PER Nuclear and cytoplasmic extraction reagents (Pierce) containing protease inhibitors and were subsequently separated on a 4-12% Bis-Tris gel (Life Technologies). Proteins (25 to 50 µg per lane) were transferred to nitrocellulose and the membrane was blocked with Casein blocker solution for 1h. Membranes were subsequently incubated overnight at 4°C with a rabbit anti-ABCG1 antibody (NB400-132; Novus) at 1:2500 and goat anti-rabbit/HRP antibody (Dako) at 1:5000. Quantification of Western blots was performed using a Kodak Image Station 440 CF with Kodak 1D Image Analysis Software (Perkin Elmer, Villebon-sur-Yvette, France).

Human liver ABCG1 detection by immunohistochemistry

Immunohistochemistry of human liver biopsies was performed as previously described[32]. Briefly, following paraffin embedding, 3-5 pm thick sections were cut and tested by the ABC (avidin-biotin complex) immunoperoxidase method. Deparaffinised sections were soaked in phosphate-buffered saline (PBS), pH 7.4, containing 3% hydrogen peroxide for 5 min at room temperature in order to eliminate endogenous peroxidase activity. After washing and incubation with normal goat serum (ABC kit, Vector Laboratories) at 1:200 for 30 min, each section was incubated at 4°C with the anti-ABCG1 antibody from Novus (NB400-132) at 1:100 for 12h followed by incubation with biotin-labelled secondary antibody (ABC kit) at 1:200 for 30 min. Kupffer cells were visualized with anti-CD68 from Dako (CD68, Clone PG-M1) using a Fast red substrate kit. After washing, the ABC complex (ABC kit) was applied for 45 min. Brown staining was produced by 5 mm treatment with 3,3'-diaminobenzidine (DAB, 50 mg in 100 ml PBS, pH 7.4, containing 0.01% hydrogen peroxide). Counterstaining was performed with Mayer's haematoxylin. In negative controls carried out in all single and double immunostaining experiments, each primary antibody was replaced with an immunoglobulin fraction of non-immune serum.

Statistical analyses

Data are shown as mean ± SEM. Experiments were performed in triplicate and values shown represent a mean of at least three independent experiments. Comparisons of two groups were performed by a 2-tailed Student's t-test and comparisons of three or more groups by ANOVA with Newman–Keuls post-hoc test. All statistical analyses were performed using Prism software from GraphPad (San Diego, CA, USA). For lipidomics, normalized mean-center data were drawn as a clustered lipidomic array (heat map) using Multi Experiment Viewer (MeV) software version 4.9 (https://sourceforge.net/projects/mev-tm4/)[33]. Metabolites considered to vary significantly between two respective subjects were identified using Wilcoxon-Mann-Whitney non-parametric test, with $p<0.05$ as a significance threshold. The Benjamini−Hochberg correction was applied to control for false discovery rate[34] (FDR). Analysis of variance (ANOVA) was done using MeV 4.9 with a threshold of $p<0.05$. When the non-parametric test and ANOVA returned an overall level of significance of $p<0.05$

between the subjects, a Hierarchical Clustering tree (HCL) was subsequently built. Lipid features were clustered using complete linkage over the samples using Pearson correlation distance matrix.

Results.

Enhanced atheroprotective functions of HDL remodeled by human ABCG1.

In order to assess the hypothesis that ABCG1-mediated lipid remodeling of HDLs impacts their functionality, large human HDL2, the preferential lipid acceptor for ABCG1, were incubated with either CHO cells expressing the human form of ABCG1 (hABCG1)[20] or control cells for a 16h-period at 37°C and then tested for their biological activities (Figure 1A). As shown in Figure 1B, HDL2 remodeled by hABCG1 exhibited significantly elevated capacity to promote free cholesterol efflux (+15%, $p<0.05$) from primary culture of human macrophages (HMDM) as compared to HDL2 incubated with control cells. In addition, anti-inflammatory activity of HDL2 was greatly enhanced following the remodeling by ABCG1 as testified by the marked decrease of the secretion of pro-inflammatory cytokines interleukin-6 (-60%, $p<0.01$; Fig. 1C) and tumor necrosis factor-α (-60%, $p<0.05$; Fig. 1D) for 8 hours in the media of LPS-treated HMDM in comparison to control HDL2. Taken together, these results indicated that the remodeling of large HDLs by human ABCG1 improves their atheroprotective properties.

Functional ABCG1 is expressed in human hepatocytes

Liver is a key organ in HDL biology since it contributes to HDL biogenesis and metabolism through the hepatic expression of specific transporters, receptors and plasma enzymes. Previous studies reported poor hepatic expression of Abcg1 in rodents, which was apparently restricted to Kupffer cells (KC)[21,35]. Analysis of the expression of Abcg1 in hepatocytes and KC isolated from the liver of C57BL/6 mice fed a chow diet in the present study confirmed previous observations as we observed 19-fold higher *Abcg1* mRNA levels in KC relative to hepatocytes (Figure 2A). No data are however available in the literature about the ABCG1 expression in human liver. Using immunohistochemistry experiments from biopsies of human livers, we were able to detect a strong expression of ABCG1 in hepatocytes as well as in macrophages identified by CD68 staining (Figure 2B), thereby contrasting to what was observed in mice. Next, to determine if ABCG1 was functional in human hepatocytes, lipid efflux experiments were conducted in primary human hepatocytes (PHH) in which ABCG1 was knocked down (ABCG1 KD), or not (Control), by RNAi (Figure 2C-D). We observed that cholesterol efflux to HDL was significantly reduced in ABCG1 KD PHH as compared to control cells (Figure 2C). Similar results were obtained using

the human hepatocellular carcinoma cell line Hep3B (Supplemental Figure 2). As a whole, these data demonstrated that ABCG1 was robustly expressed and exhibited a functional lipid efflux activity in human hepatocytes.

Hepatic expression of hABCG1 in mice enhances the cholesterol efflux capacity of HDL

To assess whether the hepatic expression of ABCG1 may improve the functionality of HDL, human ABCG1 was transiently expressed through systemic injection of a hABCG1 coding plasmid in double transgenic mice expressing human ApoB and cholesterol ester transfer protein (CETP; hApoB/CETP mice) who display plasma lipoprotein profile similar to that of normolipidemic humans[36]. As shown in Figure 3A, high amounts of human *ABCG1* mRNA levels were detected in livers of hApoB/CETP mice 6 days following the injection of the hABCG1 coding plasmid as compared to mice injected with the control plasmid. Isolation of hepatocytes (Fig. 3B) and KC (Fig. 3C) from murine livers indicated that hepatic expression of hABCG1 mostly reflected hABCG1 expression in hepatocytes whereas the latter was undetectable in KC. Analysis of plasma lipid levels indicated that hABCG1 expression in hApoB/CETP mice was without significant effect on both total cholesterol (Fig. 3D) and HDL-C (Fig. 3E) levels when compared to animals injected with the control plasmid. Interestingly, plasma from mice expressing hABCG1 exhibited significantly higher capacity to promote cholesterol efflux from human THP-1 macrophages than that from control animals (+36%, $p<0.05$; Figure 3F). A similar effect was observed when plasma depleted in ApoB-containing lipoproteins was used indicating that the enhanced macrophage cholesterol efflux to the whole plasma was attributable to HDL (Figure 3G).

To explore accurately the impact of the specific hABCG1 expression on HDL remodeling and functionality, a similar experimental approach was employed in *Abcg1*$^{-/-}$ mice who do not express endogenous Abcg1. Analysis of hepatic *Abcg1* mRNA levels confirmed the predominant expression of Abcg1 in KC in *Abcg1*$^{+/+}$ mice, which was drastically reduced in littermate *Abcg1*$^{-/-}$ mice (Figure 4A). It is of note that plasma TC levels as well as the capacity of plasma to promote macrophage cholesterol efflux were unchanged between *Abcg1*$^{+/+}$ and *Abcg1*$^{-/-}$ mice (Figure 4B-C). As observed in ApoB/CETP mice, retro-orbital injection of the hABCG1 coding plasmid in *Abcg1*$^{-/-}$ mice resulted in a strong expression of human *ABCG1* mRNA in hepatocytes in comparison to mice injected with the control

plasmid (figure 4D), without affecting residual mRNA levels of endogenous murine *Abcg1*. In addition, plasma cholesterol levels (which mainly reflect those of HDL-C in C57BL/6 mice) were not altered following the expression of hABCG1 in *Abcg1*$^{-/-}$ animals (Figure 4E). Such hABCG1 expression resulted in significantly elevated capacity of plasma to promote cholesterol efflux from THP-1 macrophages (+33%, $p<0.05$; Figure 4F). Taken together, these results demonstrated that the expression of human ABCG1 in hepatocytes was accompanied by subsequent enhancement of the capacity of HDL to promote macrophage cholesterol efflux.

Expression of human ABCG1 affects the phospholipidome of HDL

To assess whether the expression of human ABCG1 impacts the HDL phospholipidome, we performed LC-ESI/MS/MS analysis on total plasma HDL isolated from *Abcg1*$^{-/-}$ mice 7 days following the injection with either the hABCG1 coding vector or the control plasmid. Analysis of total lipid and protein composition (Figure 5A) as well as proportions of major phospholipid and sphingolipid classes (Figure 5B) in HDL did not reveal significant changes as a result of the expression of hABCG1 even if the abundances of both total PS and SM tended to be elevated (+24% and +14%, respectively). However, quantification of 247 lipid molecular species in HDL including 17 LPC, 12 LPE, 8 PA, 25 PC, 16 pPE, 21 PE, 15 PG, 17 PI, 19 PS, 25 ceramides (dihydro- and ceramides), 15 SM and 57 TG species (Supplemental Table 2) led us to identify 10 lipid species significantly altered in HDL isolated from mice injected with the hABCG1 plasmid as compared to control mice (FDR corrected at <0,05; Figure 5C and Supplemental Figure 3). Among them, the abundances of 3 lipid species (PI (38:6), PE (16:0p/20:4) and PS (32:0)) were increased, whereas those of 7 lipid species (PA (36:2), PI 36:2), PE (36:5), PG (36:1), PG (36:2), PC (36:2) and Cer (d18:0-24:0)) were reduced in HDL from mice expressing human ABCG1. Herewith, we demonstrated that the expression of human ABCG1 in hepatocytes was accompanied by a modification of the HDL phospholipidome in mice.

Impact of the functional rs1378577 *ABCG1* polymorphism on the phospholipidome and macrophage cholesterol efflux capacity of HDL

In order to translate our findings in the context of human physiopathology, we took advantage of the functional rs1378577 *ABCG1* SNP located in the promoter region, which was reported by us to

modulate *ABCG1* expression[22,37]. Indeed, the transient transfection of human HepG2 cells revealed that the expression of the human *ABCG1* promoter containing the T allele of the rs1378577 was significantly increased as compared to that containing the G allele (Figure 6A). In addition, we previously genotyped the rs1378577 SNP in a population of 396 normolipidemic individuals[25] and females homozygous for either the frequent T (T/T, n=40) or the rare G (G/G, n=28) allele were selected for the study. No difference in plasma lipid levels, including HDL-C, was observed between subjects carrying either the T/T (n=40) or the G/G (n=28) genotype (Supplemental Table 1). In agreement with our *in vivo* data obtained in different mouse models, the capacity of plasma of T/T carriers (displaying high *ABCG1* expression) to promote macrophage cholesterol efflux was significantly elevated (+15%, $p<0.05$) relative to plasma of G/G carriers (featuring low *ABCG1* expression; Figure 6B). The capacity of HDL2 isolated from women subjects carrying the T/T genotype was higher than that from their counterparts carrying the G/G genotype (Figure 6C). To determine if this increase was associated with ABCG1-mediated remodeling of the HDL2 phospholipidome, abundances of 10 lipid species specifically altered in mouse HDL by human ABCG1 (Figure 5C) were quantified by LC-ESI/MS/MS in HDL2 particles from T/T and G/G individuals. In agreement with what was observed in mice, the abundances of 6 (PA (36:2), PI (38:6), PI (36:2), PE (36:5), PG (36:1), PG (36:2)) out of 10 species (with PE (16:0p/20:4) and PS (32:0) being not detected) were significantly reduced in subjects exhibiting high ABCG1 expression (T/T carriers) as compared to those with low ABCG1 expression (G/G carriers; Figure 6D-K). These data led us to conclude that elevated expression of ABCG1 in healthy normolipidemic women remodeled the HDL2 phospholipidome in parallel with enhancement of HDL capacity to promote macrophage cholesterol efflux.

Modulation of the HDL phospholipidome by human ABCG1 mostly results from its expression in hepatocytes

Our *in vivo* findings in both mice and humans revealed a close link between the human ABCG1 expression and the phospholipidome of circulating HDL, identifying several lipid species whose HDL abundance was altered by ABCG1. However, it was not clear at this stage whether this alteration directly resulted from the action of ABCG1 at a cellular level, probably in hepatocytes, or reflected

further remodeling of HDL particles in the intravascular compartment. To address this question, human HDL2 were incubated with both control and ABCG1 KD PHH for a 16h period at 37°C and the abundance of 10 lipid species specifically altered in mouse HDL by human ABCG1 was quantified in remodeled HDL2 by LC-ESI/MS/MS. In agreement with what was observed in both mice and humans, the abundances of 5 out of 10 lipid species (with PE (16:0p/20:4) and PS (32:0) being not detected) were either elevated (PI (38:6), PA (36:2), PI (36:2), PE (36:5)) or reduced (PG (36:1)) in ABCG1 KD PHH relative to control PHH, whereas those of 3 lipid species were not altered (PG (36:2), PC (36:2) and Cer (d18:0-24:0); Figure 7). Taken together, these results strongly suggest that the ABCG1-dependent remodeling of the HDL2 phospholipidome predominantly resulted from the activity of ABCG1 in hepatocytes.

ABCG1-mediated remodeling of HDL and atherosclerosis

Finally, to assess whether the ABCG1-mediated remodeling of HDL2 particles might have an effect on atherosclerosis development, the amount of 6 lipid species (PI (38:6), PA (36:2), PI (36:2), PE (36:5), PG (36:1) and PG (36:2)) whose abundance was altered in HDL2 according to the rs1378577 *ABCG1* SNP and/or the hepatic ABCG1 expression was correlated with the measure of IMT of either common carotid artery (CCA-IMT) or common femoral artery (CFA-IMT). In a subset of individuals for which carotid and femoral ultrasonography was performed (n=12), strong and significant positive correlations were found between HDL2 content of PI (38:6) and PE (36:5) (which were both reduced by human ABCG1 expression) and CCA-IMT (PI (38:6) : $r=0.65$, $p=0.02$ and PE (36:5) : $r=0.61$, $p<0.03$) and CFA-IMT (PE (36:5) : $r=0.82$, $p=0.001$) (Figure 8). These results support the notion that remodeling of the HDL2 phospholipidome operated by ABCG1 might contribute to their antiatherogenic action.

Discussion.

The phospholipidome of HDL particles is closely linked to their biological activities and alterations of both the phospholipidome and atheroprotective functions of HDL are features of ASCVD patients[13–16]. Although mechanisms determining the composition of HDL in PL species are largely unknown, a growing body of evidences supports the notion that variations in the HDL phospholipidome may contribute to CVD risk. We herein identified membrane ABCG1 transporter as being an important determinant of the HDL phospholipidome and functions with potential implications in atherosclerosis.

Beyond its known role in cellular cholesterol efflux to extracellular acceptors such as HDL, ABCG1 was equally reported to promote the export of other classes of lipids including phospholipids and sphingomyelin[14]. Using complementary *in vitro* and *in vivo* approaches, we demonstrated that the expression of hepatic ABCG1 led to significant modifications of the content of phospholipid and sphingolipid molecular species in HDL, with the identification of a set of molecules which represents a signature of such ABCG1-mediated remodeling. Unexpectedly, PC content of HDL was not affected by ABCG1 expression even if several studies reported that ABCG1 promoted cellular PC efflux to HDL. However, Kobayashi et al. reported using HEK293 cells stably expressing ABCG1 that human ABCG1 preferentially secretes SM in extracellular media[18]. In addition, a similar comment can be made regarding the cholesterol content of HDL which was not affected by ABCG1 expression while its role in the export of cholesterol from numerous cell types, including hepatocytes as investigated in the present study, was frequently demonstrated. In addition, the expression of ABCG1 in both humans and mice was without effect on circulating HDL-C levels[21,37]. Thus, although PC was the most abundant PL class in HDL, we herein demonstrated that ABCG1-mediated remodeling of HDL predominantly involves less abundant PL classes. Taken together, these findings indicate that lipid efflux activity of ABCG1 leads to subtle changes in the lipid composition of HDL without any major alteration of their lipid content. Interestingly, analysis of the HDL lipidome by LC-ESI/MS/MS revealed that the HDL remodeled by ABCG1 largely revealed a relative loss of molecular lipid species rather than their gain as expected from the ABCG1-mediated PL efflux. Indeed, only 3 lipid species of plasmalogens, PS and PI were detected at a higher abundance in HDL following human ABCG1 expression, whereas the abundance of 7 lipid

species from PC, PG, PI and PE was decreased. These observations suggest that the incorporation of the three species of PS (32:0), PI (38:6) and PE (16:0p/20:4) at the HDL surface leads to the displacement of other lipid species, including PC (36:2), PA (36:2), PI (36:2), PG (36:2), PG (36:1), PE (36:5) and Cer (d18:0-24:0). Such a remodeling of HDL likely occurs at the cellular level in interaction with ABCG1 rather than in the intravascular compartment under the action of plasma enzymes, since most of these modifications were equally observed following HDL incubation with primary human hepatocytes in which ABCG1 expression was manipulated. Strikingly, lipidomic analysis of HDL in both mouse and human models revealed that the remodeling of the HDL phospholipidome by ABCG1 does not occur randomly but rather involves specific PL species containing monounsaturated or polyunsaturated medium-chain fatty acid residues of 16 to 20 carbon atoms, with a predominance of 36:2-containing species.

In the present study, the modification of the HDL phosphosphingolipidome by ABCG1 was accompanied by enhancement of its biological functions, including anti-inflammatory activity and capacity to promote macrophage cholesterol efflux; the latter is robustly associated with ASCVD[5–7]. Although it is difficult to univocally conclude without conducting appropriate structure-function studies that such a modification of the HDL phosphosphingolipidome could fully account for the observed effect of ABCG1 on HDL function, the PL remodeling of HDL induced by ABCG1 is however consistent with its elevated biological activity. Indeed, we previously demonstrated that enrichment of HDL particles in PS was positively correlated to all metrics of HDL functionality, including HDL capacity to promote macrophage cholesterol efflux[11]. Moreover, we demonstrated that PS-supplemented reconstituted HDL (rHDL) exhibited enhanced macrophage cholesterol efflux activity and anti-inflammatory properties *in vitro* and *in vivo*[38]. Plasmalogens are known to be potent antioxidant and antiapoptotic molecules and the plasmalogen content of HDL was reported to be inversely associated with the occurrence of stable and acute coronary artery disease[14]. Finally, the modification of the HDL content in PI molecular species induced by ABCG1 might equally impact the functionality of HDL particles, including their role in macrophage cholesterol efflux and reverse cholesterol transport[39]. Interestingly, reduced content of plasmalogen PE together with increased content of PI are features of

HDL from patients with metabolic syndrome[40], diabetes and dyslipidemia[41]. More strikingly, studies conducting lipidomic analyses of HDL from patients at high CV risk support the hypothesis that modifications of the HDL phosphosphingolipidome by ABCG1 plays an important role in their functionality. Thus, dysfunctional large HDL from ApoA-I deficient patients were enriched in Cer (d18:0-24:0), PI (36:2), PA (36:2), PG (36:1) and PG (36:2)[16], the lipid species being specifically depleted by human ABCG1 in our study. Moreover, PA (36:2), the common precursor of PI (36:2), PC (36:2), and PG (36:2), was enriched in large HDL from patients with myocardial infarction relative to control normolipidemic HDL[42]. Although the analysis of the frequent functional *ABCG1* SNP rs1378577 in a population of normolipidemic women did not reveal its effect on PC (36:2) content of HDL2 in the present study, it is noteworthy that PC (36:2) is one of the most abundant PC species found in human atherosclerotic lesions and that the distribution of PC (36:2) in plasma reflects that in the human lesions[43].

Among the molecular species of PL specifically targeted by ABCG1 in HDL, our *in vitro* and *in vivo* experiments led us to uncover that the loss of PE (36:5) in HDL consecutive to the remodeling induced by hepatic ABCG1 might contribute to the atheroprotective function of HDL. Indeed, PE (36:5) content in large HDL was strongly and positively correlated with atherosclerosis development assessed by both CCA-IMT and CFA-IMT in normolipidemic women. The observation that the abundance of PE (36:5) in HDL was increased following incubation with ABCG1 KD PHH in comparison to control cells indicates that PL efflux mediated by hepatic ABCG1 reduces (PE 36:5) content of HDL. Consistent with this conclusion, we observed that HDL isolated from mice expressing human ABCG1 in the liver or from human TT carriers for rs1378577 (associated with high ABCG1 expression) were depleted in PE (36:5). Interestingly, the deleterious role of PE (36:5) in CVD is supported by previous lipidomic analyses of plasma from control individuals and patients with CVD. Thus, plasma concentrations of PE (36:5) were significantly higher in patients with stable CAD than in control individuals when 305 lipids were quantified in 220 individuals using LC-ESI/MS/MS[13]. Even more strikingly, quantification of 135 lipids in 685 plasma samples from the prospective population-based Bruneck Study identified PE (36:5) among only three lipid species displaying the strongest predictive value for CVD. Moreover, inclusion of PE

(36:5) on top of traditional risk factors resulted in improved risk prediction and classification in this cohort[44]. Taken together, these findings suggest that PE (36:5) content of HDL, which is modulated by ABCG1 expression, might contribute to the development of ASCVD. Because functionally defective HDL is typically observed in patients at high CVD risk[45], we propose that an elevation in PE (36:5) content in HDL particles might alter their functionality by affecting receptor-dependent or independent cell-HDL interaction and/or intracellular signaling cascades triggered by HDL[46]. In addition, it is noteworthy that PE (36:5) may contain arachidonic acid (AA, 20:4) which is a key bioactive lipid species involved in inflammatory processes. As a result, PE (36:5) carried by HDL may constitute a source of AA in inflammatory cells such as macrophages, thereby contributing to the intra-lesion inflammation, through the production of prostaglandins and leukotrienes, and atherosclerosis development[47]. Interestingly, ABCG1 expression predominantly depleted HDL in 36:2 molecular species of PA (36:2), PI (36:2), PG (36:2) and PC (36:2) containing the essential linoleic acid (18:2), a precursor of AA. Future investigations are needed to assess potential impact of PE (36:5) on biological activities of HDL and to determine as to whether PE (36:5) content of HDL could represent a biomarker of ASCVD.

As a whole, our findings lead us to propose that hepatic ABCG1 expression induces selective redistribution of PL molecular species in HDL and, through this pathway contributes to antiatherogenic function of HDL. As a corollary, it can be anticipated that stimulation of ABCG1 expression in the liver could enhance the atheroprotective function of HDL, such as its capacity to promote macrophage cholesterol efflux, and thereby prevent or limit the development of atherosclerosis especially in women. Although these observations need to be confirmed in larger cohorts of women and transposed to men, our findings are of major interest since the ASCVD risk is underestimated in women and that important sex differences exist in the relation between HDL and atherosclerosis[48,49].

Although recent studies suggested that variations in the HDL phospholipidome might contribute to CVD risk[13–16], the present study uncovers a pathway governed by ABCG1 that plays important role in the PL remodeling of HDL with consequences for their functionality and atherosclerosis. In addition, our study identifies molecular lipid species in HDL that can serve as

biomarkers of HDL-mediated atheroprotection and ASCVD, providing new insights into the formulation of reconstituted HDL for therapeutic use[50].

Acknowledgements.

None.

Sources of funding.

This work was financially supported by INSERM, Sorbonne Université and the Fondation de France. L.M. Hardy, M. Olivier and E.F. Villard were recipients of a doctoral contract from Sorbonne Université.

Disclosures.

None.

References.

1. Gordon T, Castelli WP, Hjortland MC, Kannel WB, Dawber TR. High density lipoprotein as a protective factor against coronary heart disease. The Framingham Study. *Am J Med*. 1977;62:707–714.

2. Castelli WP, Garrison RJ, Wilson PW, Abbott RD, Kalousdian S, Kannel WB. Incidence of coronary heart disease and lipoprotein cholesterol levels. The Framingham Study. *JAMA*. 1986;256:2835–2838.

3. Ko DT, Alter DA, Guo H, Koh M, Lau G, Austin PC, Booth GL, Hogg W, Jackevicius CA, Lee DS, Wijeysundera HC, Wilkins JT, Tu JV. High-Density Lipoprotein Cholesterol and Cause-Specific Mortality in Individuals Without Previous Cardiovascular Conditions: The CANHEART Study. *J Am Coll Cardiol*. 2016;68:2073–2083.

4. Camont L, Chapman MJ, Kontush A. Biological activities of HDL subpopulations and their relevance to cardiovascular disease. *Trends Mol Med*. 2011;17:594–603.

5. Khera AV, Cuchel M, de la Llera-Moya M, Rodrigues A, Burke MF, Jafri K, French BC, Phillips JA, Mucksavage ML, Wilensky RL, Mohler ER, Rothblat GH, Rader DJ. Cholesterol efflux capacity, high-density lipoprotein function, and atherosclerosis. *N Engl J Med*. 2011;364:127–135.

6. Rohatgi A, Khera A, Berry JD, Givens EG, Ayers CR, Wedin KE, Neeland IJ, Yuhanna IS, Rader DR, de Lemos JA, Shaul PW. HDL cholesterol efflux capacity and incident cardiovascular events. *N Engl J Med*. 2014;371:2383–2393.

7. Guerin M, Silvain J, Gall J, Darabi M, Berthet M, Frisdal E, Hauguel-Moreau M, Zeitouni M, Kerneis M, Lattuca B, Brugier D, Collet J-P, Lesnik P, Montalescot G. Association of Serum Cholesterol Efflux Capacity With Mortality in Patients With ST-Segment Elevation Myocardial Infarction. *J Am Coll Cardiol*. 2018;72:3259–3269.

8. Rader DJ, Hovingh GK. HDL and cardiovascular disease. *Lancet*. 2014;384:618–625.

9. Davidson WS, Thompson TB. The structure of apolipoprotein A-I in high density lipoproteins. *J Biol Chem*. 2007;282:22249–22253.

10. Rosenson RS, Brewer HB, Chapman MJ, Fazio S, Hussain MM, Kontush A, Krauss RM, Otvos JD, Remaley AT, Schaefer EJ. HDL measures, particle heterogeneity, proposed nomenclature, and relation to atherosclerotic cardiovascular events. *Clin Chem*. 2011;57:392–410.

11. Camont L, Lhomme M, Rached F, Le Goff W, Nègre-Salvayre A, Salvayre R, Calzada C, Lagarde M, Chapman MJ, Kontush A. Small, dense high-density lipoprotein-3 particles are enriched in negatively charged phospholipids: relevance to cellular cholesterol efflux, antioxidative, antithrombotic, anti-inflammatory, and antiapoptotic functionalities. *Arterioscler Thromb Vasc Biol*. 2013;33:2715–2723.

12. Rached F, Santos RD, Camont L, Miname MH, Lhomme M, Dauteuille C, Lecocq S, Serrano CV, Chapman MJ, Kontush A. Defective functionality of HDL particles in familial apoA-I deficiency: relevance of alterations in HDL lipidome and proteome. *J Lipid Res*. 2014;55:2509–2520.

13. Meikle PJ, Wong G, Tsorotes D, Barlow CK, Weir JM, Christopher MJ, MacIntosh GL, Goudey B, Stern L, Kowalczyk A, Haviv I, White AJ, Dart AM, Duffy SJ, Jennings GL, Kingwell BA. Plasma lipidomic analysis of stable and unstable coronary artery disease. *Arterioscler Thromb Vasc Biol*. 2011;31:2723–2732.

14. Sutter I, Velagapudi S, Othman A, Riwanto M, Manz J, Rohrer L, Rentsch K, Hornemann T, Landmesser U, von Eckardstein A. Plasmalogens of high-density lipoproteins (HDL) are associated with coronary artery disease and anti-apoptotic activity of HDL. *Atherosclerosis*. 2015;241:539–546.

15. Horter MJ, Sondermann S, Reinecke H, Bogdanski J, Woltering A, Kerber S, Breithardt G, Assmann G, Von Eckardstein A. Associations of HDL phospholipids and paraoxonase activity with coronary heart disease in postmenopausal women. *Acta Physiol Scand*. 2002;176:123–130.

16. Zakiev E, Rached F, Lhomme M, Darabi-Amin M, Ponnaiah M, Becker PH, Therond P, Serrano CV, Santos RD, Chapman MJ, Orekhov A, Kontush A. Distinct phospholipid and sphingolipid species are linked to altered HDL function in apolipoprotein A-I deficiency. *J Clin Lipidol*. 2019;13:468-480.e8.

17. Hardy LM, Frisdal E, Le Goff W. Critical Role of the Human ATP-Binding Cassette G1 Transporter in Cardiometabolic Diseases. *Int J Mol Sci*. 2017;18.

18. Kobayashi A, Takanezawa Y, Hirata T, Shimizu Y, Misasa K, Kioka N, Arai H, Ueda K, Matsuo M. Efflux of sphingomyelin, cholesterol, and phosphatidylcholine by ABCG1. *J Lipid Res*. 2006;47:1791–1802.

19. Wang N, Ranalletta M, Matsuura F, Peng F, Tall AR. LXR-induced redistribution of ABCG1 to plasma membrane in macrophages enhances cholesterol mass efflux to HDL. *Arterioscler Thromb Vasc Biol*. 2006;26:1310–1316.

20. Gelissen IC, Harris M, Rye K-A, Quinn C, Brown AJ, Kockx M, Cartland S, Packianathan M, Kritharides L, Jessup W. ABCA1 and ABCG1 synergize to mediate cholesterol export to apoA-I. *Arterioscler Thromb Vasc Biol*. 2006;26:534–540.

21. Kennedy MA, Barrera GC, Nakamura K, Baldán A, Tarr P, Fishbein MC, Frank J, Francone OL, Edwards PA. ABCG1 has a critical role in mediating cholesterol efflux to HDL and preventing cellular lipid accumulation. *Cell Metab*. 2005;1:121–131.

22. Frisdal E, Le Lay S, Hooton H, Poupel L, Olivier M, Alili R, Plengpanich W, Villard EF, Gilibert S, Lhomme M, Superville A, Miftah-Alkhair L, Chapman MJ, Dallinga-Thie GM, Venteclef N, Poitou C, Tordjman J, Lesnik P, Kontush A, Huby T, Dugail I, Clement K, Guerin M, Le Goff W. Adipocyte ATP-binding cassette G1 promotes triglyceride storage, fat mass growth, and human obesity. *Diabetes*. 2015;64:840–855.

23. Bellanger N, Orsoni A, Julia Z, Fournier N, Frisdal E, Duchene E, Bruckert E, Carrie A, Bonnefont-Rousselot D, Pirault J, Saint-Charles F, Chapman MJ, Lesnik P, Le Goff W, Guerin M. Atheroprotective reverse cholesterol transport pathway is defective in familial hypercholesterolemia. *Arterioscler Thromb Vasc Biol*. 2011;31:1675–1681.

24. Catalano G, Duchene E, Julia Z, Le Goff W, Bruckert E, Chapman MJ, Guerin M. Cellular SR-BI and ABCA1-mediated cholesterol efflux are gender-specific in healthy subjects. *J Lipid Res*. 2008;49:635–643.

25. Villard EF, EI Khoury P, Frisdal E, Bruckert E, Clement K, Bonnefont-Rousselot D, Bittar R, Le Goff W, Guerin M. Genetic determination of plasma cholesterol efflux capacity is gender-specific and independent of HDL-cholesterol levels. *Arterioscler Thromb Vasc Biol*. 2013;33:822–828.

26. Gall J, Frisdal E, Bittar R, Le Goff W, Bruckert E, Lesnik P, Guerin M, Giral P. Association of Cholesterol Efflux Capacity With Clinical Features of Metabolic Syndrome: Relevance to Atherosclerosis. *J Am Heart Assoc*. 2016;5.

27. Ejsing CS, Duchoslav E, Sampaio J, Simons K, Bonner R, Thiele C, Ekroos K, Shevchenko A. Automated identification and quantification of glycerophospholipid molecular species by multiple precursor ion scanning. *Anal Chem*. 2006;78:6202–6214.

28. Frisdal E, Lesnik P, Olivier M, Robillard P, Chapman MJ, Huby T, Guerin M, Le Goff W. Interleukin-6 protects human macrophages from cellular cholesterol accumulation and attenuates the proinflammatory response. *J Biol Chem*. 2011;286:30926–30936.

29. Silvie O, Rubinstein E, Franetich J-F, Prenant M, Belnoue E, Rénia L, Hannoun L, Eling W, Levy S, Boucheix C, Mazier D. Hepatocyte CD81 is required for Plasmodium falciparum and Plasmodium yoelii sporozoite infectivity. *Nat Med*. 2003;9:93–96.

30. El Khoury P, Waldmann E, Huby T, Gall J, Couvert P, Lacorte J-M, Chapman J, Frisdal E, Lesnik P, Parhofer KG, Le Goff W, Guerin M. Extended-Release Niacin/Laropiprant Improves Overall Efficacy of Postprandial Reverse Cholesterol Transport. *Arterioscler Thromb Vasc Biol*. 2016;36:285–294.

31. Larrede S, Quinn CM, Jessup W, Frisdal E, Olivier M, Hsieh V, Kim M-J, Van Eck M, Couvert P, Carrie A, Giral P, Chapman MJ, Guerin M, Le Goff W. Stimulation of cholesterol efflux by LXR agonists in cholesterol-loaded human macrophages is ABCA1-dependent but ABCG1-independent. *Arterioscler Thromb Vasc Biol*. 2009;29:1930–1936.

32. Bobryshev YV, Lord RS. S-100 positive cells in human arterial intima and in atherosclerotic lesions. *Cardiovasc Res*. 1995;29:689–696.

33. Saeed AI, Sharov V, White J, Li J, Liang W, Bhagabati N, Braisted J, Klapa M, Currier T, Thiagarajan M, Sturn A, Snuffin M, Rezantsev A, Popov D, Ryltsov A, Kostukovich E, Borisovsky I, Liu Z, Vinsavich A, Trush V, Quackenbush J. TM4: a free, open-source system for microarray data management and analysis. *BioTechniques*. 2003;34:374–378.

34. Benjamini Y, Hochberg Y. Controlling the False Discovery Rate: A Practical and Powerful Approach to Multiple Testing. *Journal of the Royal Statistical Society Series B (Methodological)*. 1995;57:289–300.

35. Hoekstra M, Kruijt JK, Van Eck M, Van Berkel TJC. Specific gene expression of ATP-binding cassette transporters and nuclear hormone receptors in rat liver parenchymal, endothelial, and Kupffer cells. *J Biol Chem*. 2003;278:25448–25453.

36. Grass DS, Saini U, Felkner RH, Wallace RE, Lago WJ, Young SG, Swanson ME. Transgenic mice expressing both human apolipoprotein B and human CETP have a lipoprotein cholesterol distribution similar to that of normolipidemic humans. *J Lipid Res*. 1995;36:1082–1091.

37. Olivier M, Tanck MW, Out R, Villard EF, Lammers B, Bouchareychas L, Frisdal E, Superville A, Van Berkel T, Kastelein JJ, Eck MV, Jukema JW, Chapman MJ, Dallinga-Thie GM, Guerin M, Le Goff W. Human ATP-binding cassette G1 controls macrophage lipoprotein lipase bioavailability and promotes foam cell formation. *Arterioscler Thromb Vasc Biol*. 2012;32:2223–2231.

38. Kontush A, Tubeuf E, Le Goff W, Dauteuille C, Guillas-Baudouin I, Lhomme M, Patel M, Huby T, Chapman MJ, Rye KA, Lesnik P. Phosphatidylserine potently enhances anti-inflammatory activities of reconstituted HDL. *Atherosclerosis*. 2015;241:e30.

39. Burgess JW, Boucher J, Neville TA-M, Rouillard P, Stamler C, Zachariah S, Sparks DL. Phosphatidylinositol promotes cholesterol transport and excretion. *J Lipid Res*. 2003;44:1355–1363.

40. Denimal D, Nguyen A, Pais de Barros J-P, Bouillet B, Petit J-M, Vergès B, Duvillard L. Major changes in the sphingophospholipidome of HDL in non-diabetic patients with metabolic syndrome. *Atherosclerosis*. 2016;246:106–114.

41. Ståhlman M, Fagerberg B, Adiels M, Ekroos K, Chapman JM, Kontush A, Borén J. Dyslipidemia, but not hyperglycemia and insulin resistance, is associated with marked alterations in the HDL lipidome in type 2 diabetic subjects in the DIWA cohort: impact on small HDL particles. *Biochim Biophys Acta*. 2013;1831:1609–1617.

42. Zakiev E, Ma F, Rached F, Lhomme M, Sukhorukov V, Serrano CV, Santos RD, Chapman MJ, Orekhov A, Kontush A. Unsaturated, low-abundant species of HDL (Lyso)phospholipids are most affected by ST segment elevation myocardial infarction. *Atherosclerosis*. 2018;275:e56–e57.

43. Stegemann C, Drozdov I, Shalhoub J, Humphries J, Ladroue C, Didangelos A, Baumert M, Allen M, Davies AH, Monaco C, Smith A, Xu Q, Mayr M. Comparative lipidomics profiling of human atherosclerotic plaques. *Circ Cardiovasc Genet*. 2011;4:232–242.

44. Stegemann C, Pechlaner R, Willeit P, Langley SR, Mangino M, Mayr U, Menni C, Moayyeri A, Santer P, Rungger G, Spector TD, Willeit J, Kiechl S, Mayr M. Lipidomics profiling and risk of cardiovascular disease in the prospective population-based Bruneck study. *Circulation*. 2014;129:1821–1831.

45. Rosenson RS, Brewer HB, Ansell BJ, Barter P, Chapman MJ, Heinecke JW, Kontush A, Tall AR, Webb NR. Dysfunctional HDL and atherosclerotic cardiovascular disease. *Nat Rev Cardiol*. 2016;13:48–60.

46. Nofer J-R. Signal transduction by HDL: agonists, receptors, and signaling cascades. *Handb Exp Pharmacol*. 2015;224:229–256.

47. Bäck M, Yurdagul A, Tabas I, Öörni K, Kovanen PT. Inflammation and its resolution in atherosclerosis: mediators and therapeutic opportunities. *Nat Rev Cardiol*. 2019;16:389–406.

48. El Khoudary SR, Ceponiene I, Samargandy S, Stein JH, Li D, Tattersall MC, Budoff MJ. HDL (High-Density Lipoprotein) Metrics and Atherosclerotic Risk in Women. *Arterioscler Thromb Vasc Biol*. 2018;38:2236–2244.

49. Fan AZ, Dwyer JH. Sex differences in the relation of HDL cholesterol to progression of carotid intima-media thickness: the Los Angeles Atherosclerosis Study. *Atherosclerosis*. 2007;195:e191-196.

50. Darabi M, Guillas-Baudouin I, Le Goff W, Chapman MJ, Kontush A. Therapeutic applications of reconstituted HDL: When structure meets function. *Pharmacol Ther*. 2016;157:28–42.

Figures.

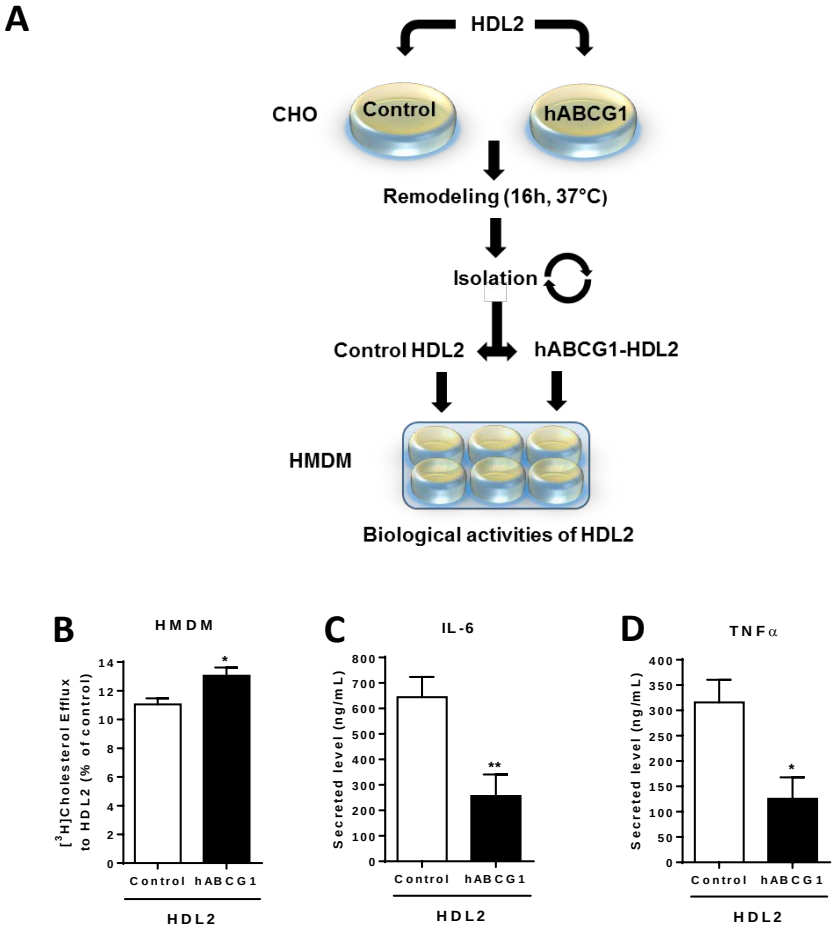

Figure 1. **Human ABCG1 expression enhanced atheroprotective functions of HDL.** A. Remodeling of HDL by ABCG1 was achieved by the incubation of large human HDL2 with CHO cells stably expressing (hABCG1) or not (Control) the human *ABCG1* gene. Following the incubation with CHO cells, HDL2 (Control or remodeled by ABCG1; hABCG1) were reisolated from the culture media by ultracentrifugation and tested for their capacity to promote free [^{3}H]cholesterol efflux (B) and to inhibit LPS-induced secretion of pro-inflammatory cytokines IL-6 (C) and TNFα (D) from human macrophage-derived monocyte (HMDM). Data are means ± SEM, *p<0.05 and **p<0.01 vs controls.

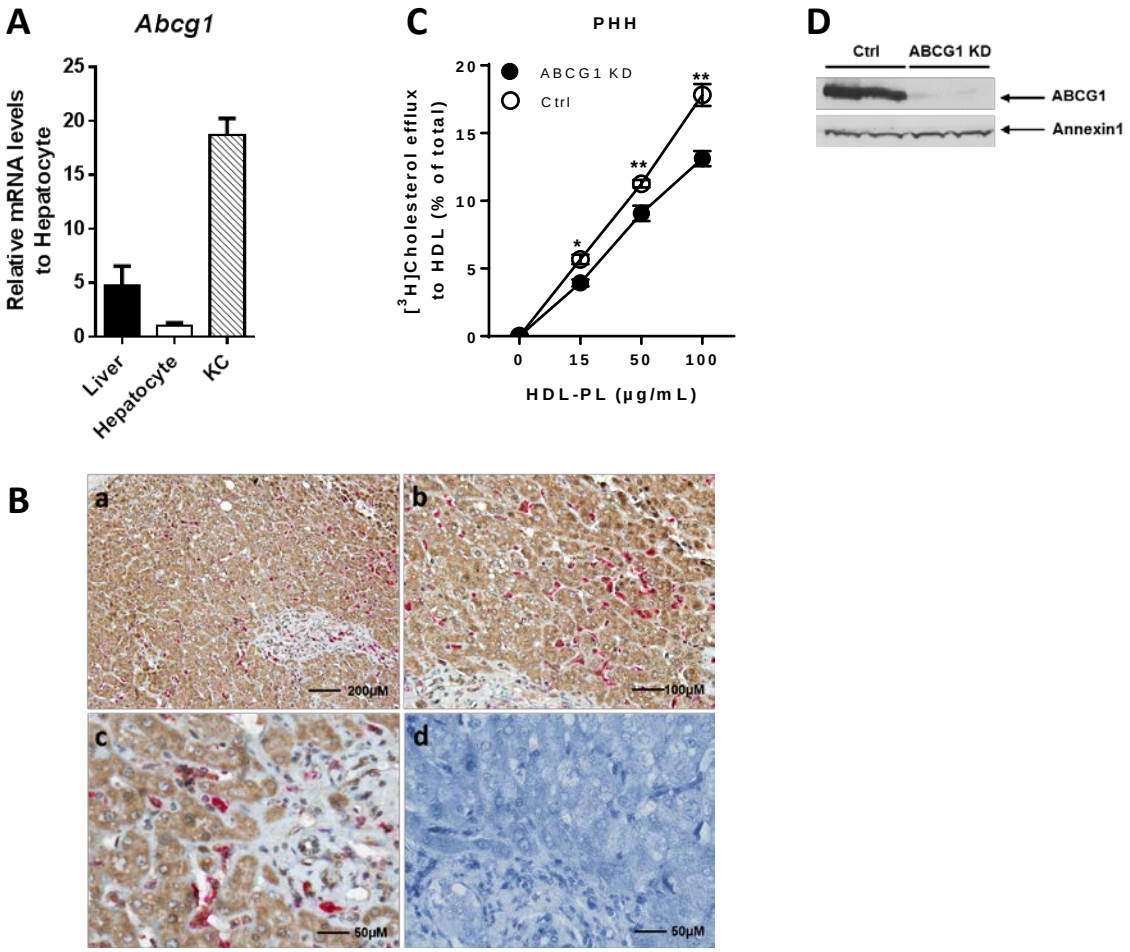

Figure 2. **Functional ABCG1 was robustly expressed in human but not in mouse hepatocytes.** A, Quantification of *Abcg1* mRNA levels in the whole liver, hepatocytes and isolated Kupffer cells (KC) from C57BL/6 mice. B, Low (a) and higher (b, c) magnification images of double immunostaining showing patterns of ABCG1 and CD68 in a human liver specimen. ABCG1 was visualized using ABC immunoperoxidase reaction (brown reaction product) while CD68 antigen was visualized using a Fast red substrate kit (rose reaction product); (d), negative control. (a-d), Counterstaining with Mayer's haematoxylin. Scale bars equal 200 µm (a), 100 µm (b) and 50 µm (c, d). C, Cellular free [^{3}H]cholesterol efflux to HDL from control (Ctrl) and ABCG1 knockdown (KD) primary human hepatocytes (PHH). D, Quantification of ABCG1 protein levels in control or ABCG1 KD PHH. Data are means ± SEM, *$p<0.05$ and **$p<0.005$ vs controls. PL, phospholipid.

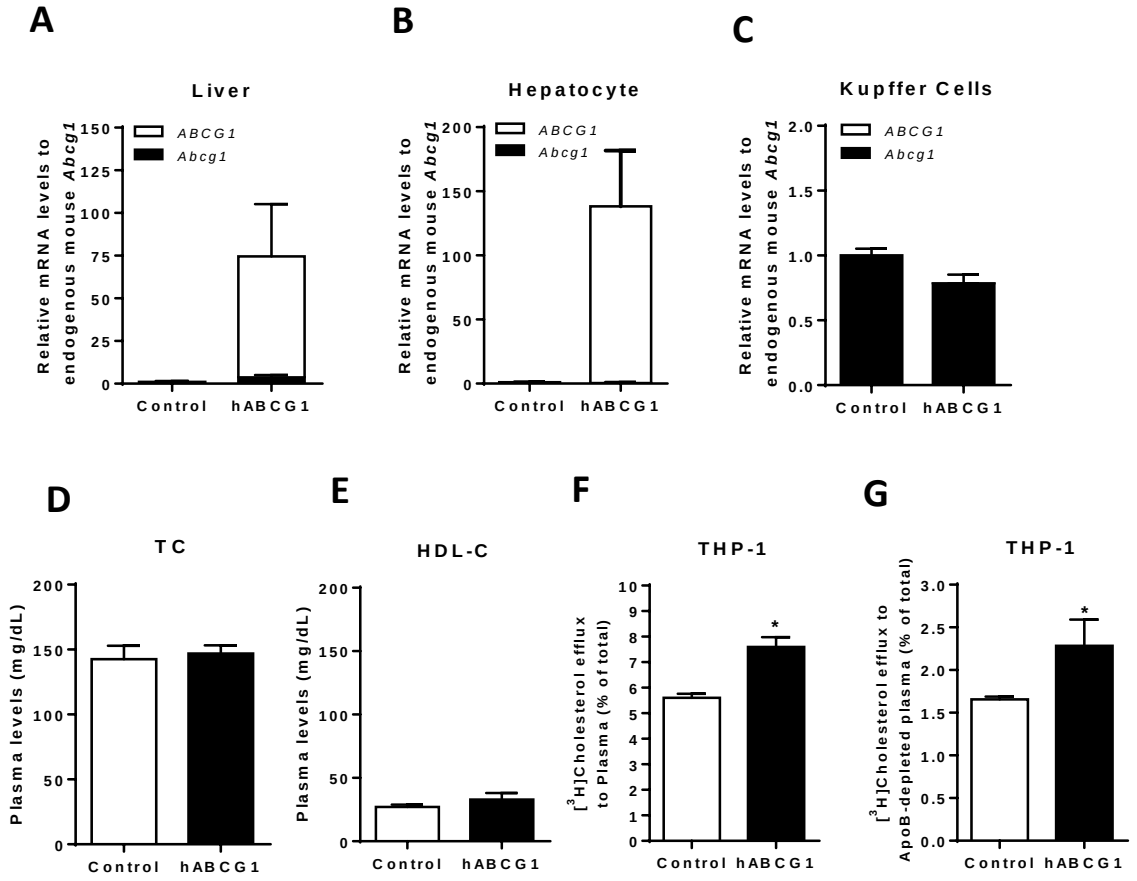

Figure 3. Enhanced capacity of HDL to promote macrophage cholesterol efflux in ApoB/CETP mice expressing human ABCG1. Quantification of mouse *Abcg1* and human *ABCG1* mRNA levels in the liver (A), hepatocytes (B) and isolated Kupffer cells (C) from ApoB/CETP mice following the injection with either a control or expressing human ABCG1 (hABCG1) vector. Plasma TC (D) and HDL-C (E) levels in control and hABCG1 ApoB/CETP mice. Capacity of whole (F) and ApoB-depleted (G) plasma from control and hABCG1 ApoB/CETP mice to promote [^{3}H]cholesterol efflux from THP-1 human macrophages. Data are means ± SEM for female mice (n=8), 10 days following the injection with either a control (Control) or expressing human ABCG1 (hABCG1) vector, *$p<0.05$ vs controls. TC, total cholesterol.

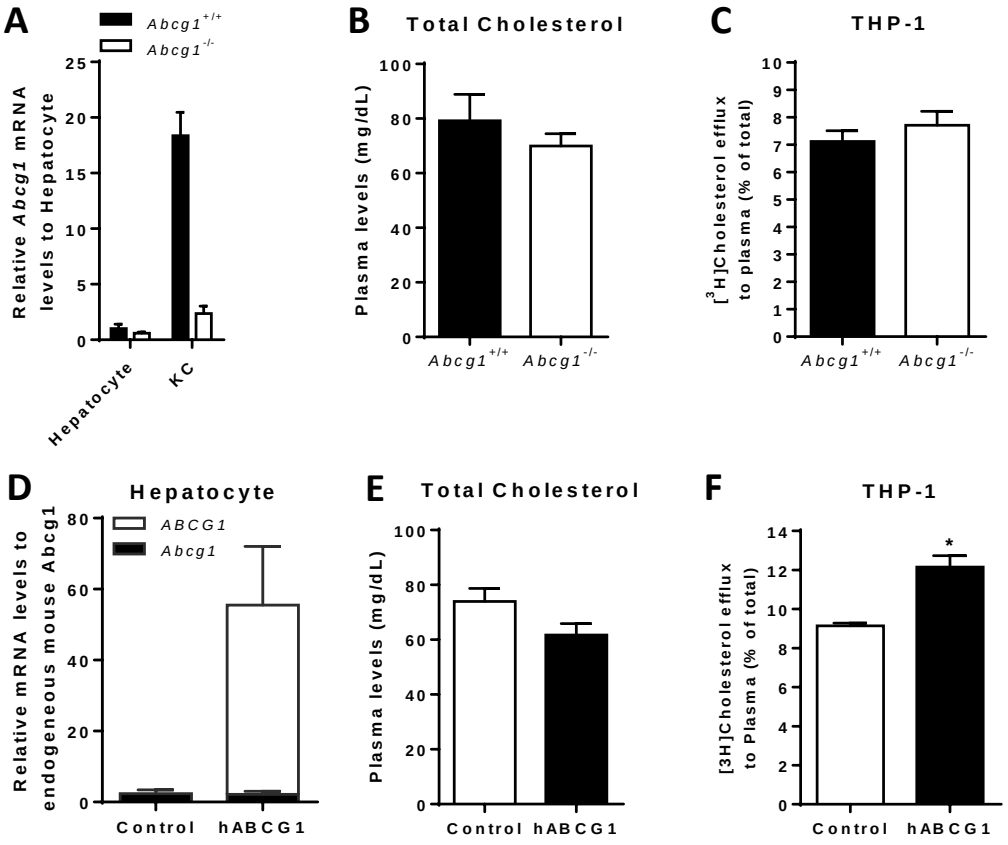

Figure 4. **Enhanced macrophage cholesterol efflux capacity of plasma from Abcg1-deficient mice expressing human ABCG1 in hepatocytes.** A, Quantification of *Abcg1* mRNA levels in hepatocytes and isolated Kupffer cells from *Abcg1*$^{+/+}$ or *Abcg1*$^{-/-}$ mice. Total cholesterol levels (B) and the capacity of plasma isolated from *Abcg1*$^{+/+}$ and *Abcg1*$^{-/-}$ mice to promote [^{3}H]Cholesterol efflux from human THP-1 macrophages (C). *D,* Quantification of murine *Abcg1* and human *ABCG1* mRNA levels in hepatocytes from *Abcg1*$^{-/-}$ mice following the injection with either a control or expressing human ABCG1 (hABCG1) vector. Total cholesterol levels (E) and the capacity of plasma obtained from control and hABCG1 *Abcg1*$^{-/-}$ mice to promote [^{3}H]Cholesterol efflux from human THP-1 macrophages (F). Data are means ± SEM for female mice (n=9) 10 days following the injection with either a control (Control) or expressing human ABCG1 (hABCG1) vector, *p<0.05 vs controls.

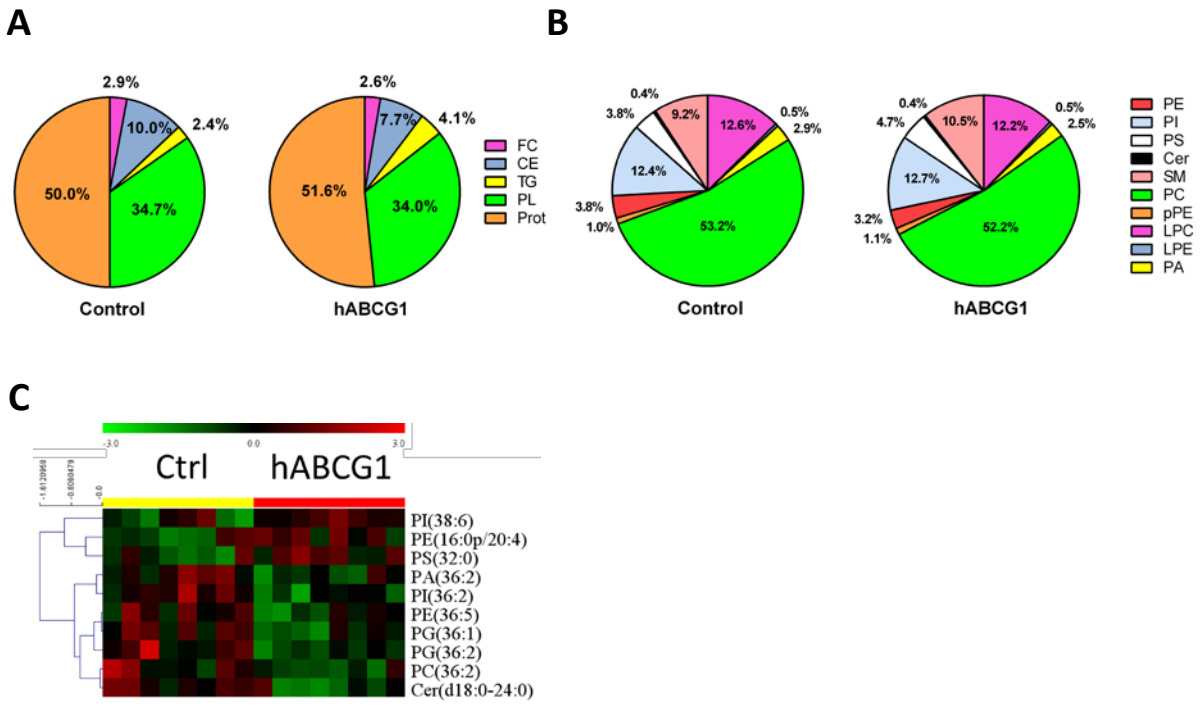

Figure 5. **Remodeling of the HDL phospholipidome following the expression of human ABCG1.** Total lipid and protein composition (A) and abundance of phospholipid and sphingolipid classes (B) of HDL from *Abcg1*$^{-/-}$ mice 10 days following the injection with either a control or expressing hABCG1 vector. C. Heat map representation of phospholipid species significantly altered following the expression of human ABCG1 ($p<0.05$ after FDR correction) in female mice (n=16) 10 days following the injection with either a control (Control) or expressing (hABCG1) vector . CE, cholesteryl ester; Cer, ceramide; FC, free cholesterol; LPC, lysophosphatidylcholine; LPE, lysophosphatidylethanolamine; PA, phosphatidic acid; PC, phosphatidylcholine; PE, phosphatidylethanolamine; PG, phosphatidylglycerol; PI, phosphatidylinositol; PL, phospholipid; pPE, plasmalogen PE; Prot, protein; PS, phosphatidylserine; SM, sphingomyelin; TG; triglyceride.

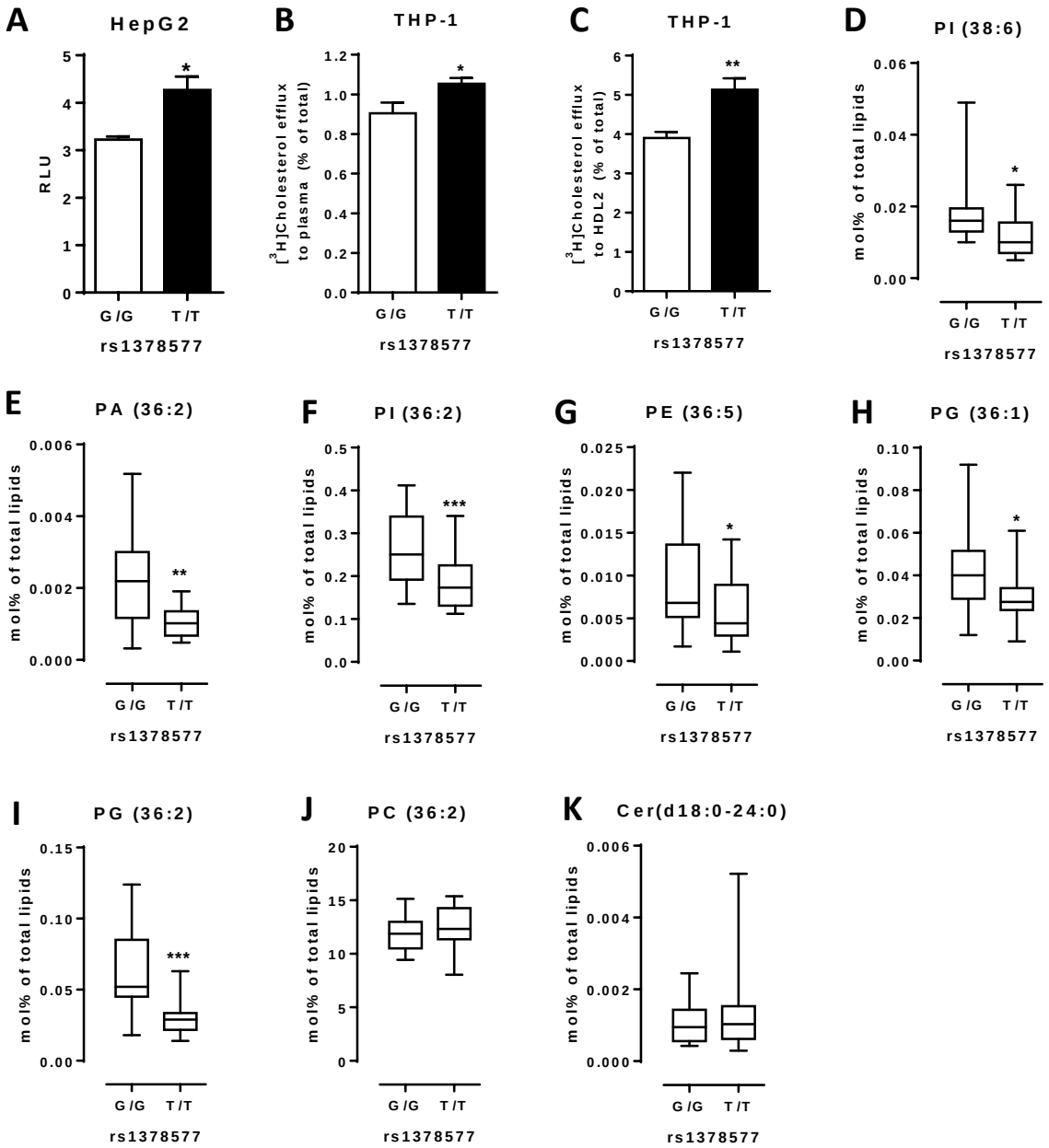

Figure 6. **Effect of the functional rs1378577 *ABCG1* polymorphism on the phospholipidome and the capacity of HDL to promote macrophage cholesterol efflux capacity.** A. Human hepatocellular carcinoma HepG2 cells were transiently transfected with a construct containing proximal 1056 bp of the human promoter with either T allele or G allele at position -134 (rs1378577). Luciferase activity was expressed in RLU after normalization for β-galactosidase activity. Capacity of plasma (B) and HDL2 (C) from normolipidemic women carrying either the G/G (low ABCG1 expression; n=28) or the T/T (high ABCG1 expression; n=40) genotype to promote free [^{3}H]Cholesterol efflux from human THP-1 macrophages. D-K, Quantification of selected phospholipid species by LC-ESI/MS/MS in HDL2 from G/G (n=21) and T/T (n=18) carriers. Data are means ± SEM, *p<0.05, **p<0.005 and ***p<0.0005 versus G/G carriers. Cer, ceramide; PA, phosphatidic acid; PC, phosphatidylcholine; PE, phosphatidylethanolamine; PG, phosphatidylglycerol; PI, phosphatidylinositol.

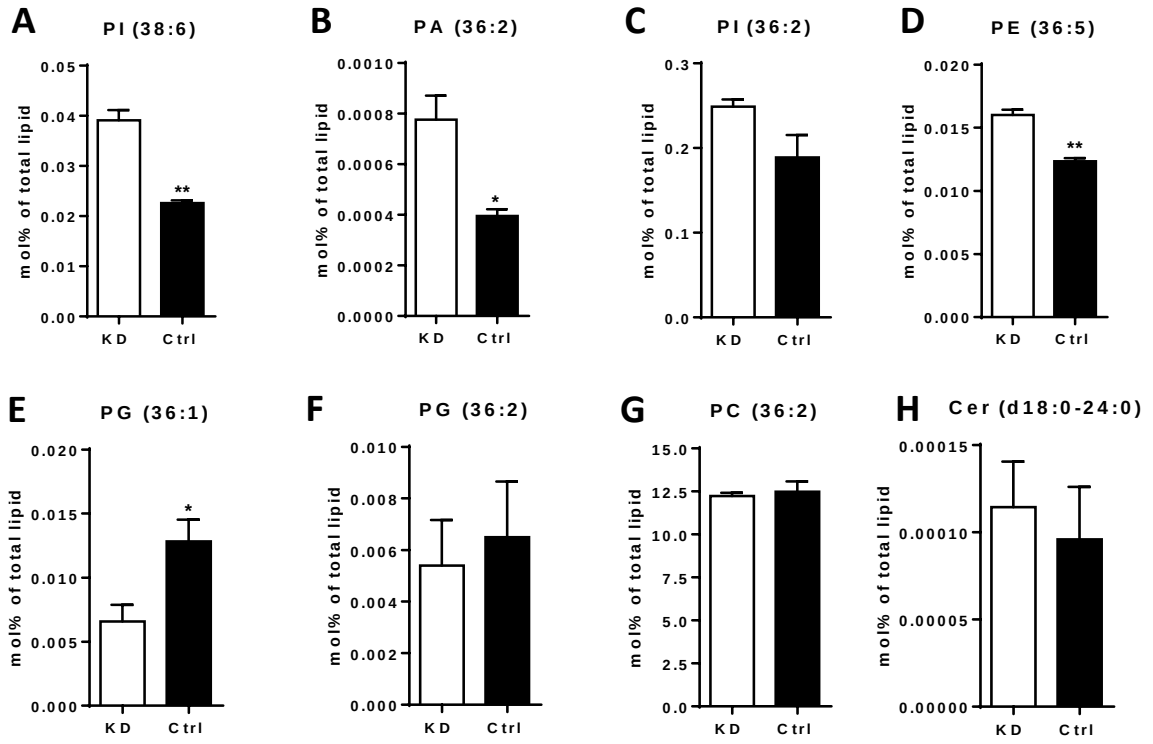

Figure 7. **Silencing of the ABCG1 expression in human primary hepatocytes recapitulated the action of ABCG1 on the HDL phospholipidome . A-D,** Quantification of selected phospholipid species by LC-MS/MS in HDL2 incubated with either control (Ctrl) or ABCG1 knockdown (KD) primary human hepatocytes. Data are means ± SEM, *p<0.05 and **p<0.005 vs controls. n=6 per group. Cer, ceramide; PA, phosphatidic acid; PC, phosphatidylcholine; PE, phosphatidylethanolamine; PG, phosphatidylglycerol; PI, phosphatidylinositol.

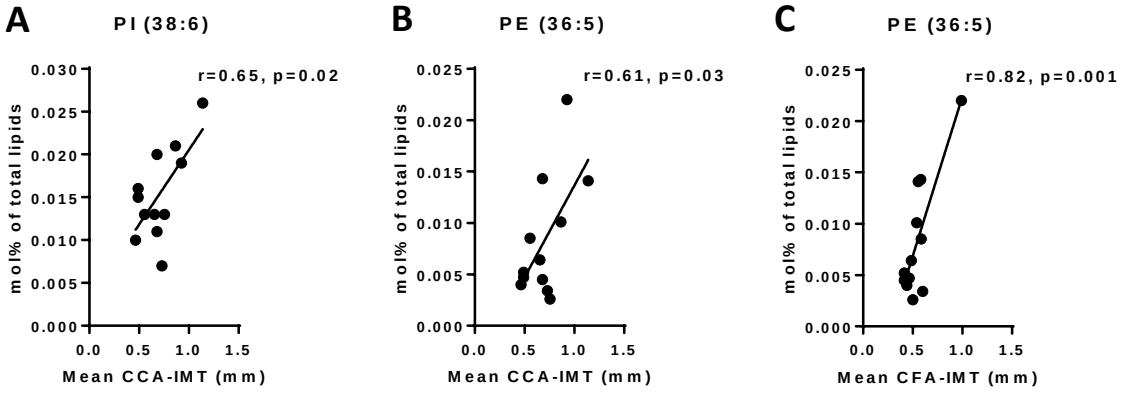

Figure 8. Remodeling of the HDL phospholipidome by ABCG1 was correlated with atherosclerosis. Correlation of HDL2 content in PI (38:6) (A) and PE (36:5) (B-C) with IMT of either the common carotid artery (CCA-IMT; A-B) or common femoral artery (CFA-IMT; C) in normolipidemic women (n=12); *r*, Pearson's correlation. PE, phosphatidylethanolamine; PI, phosphatidylinositol.

Supplemental figures.

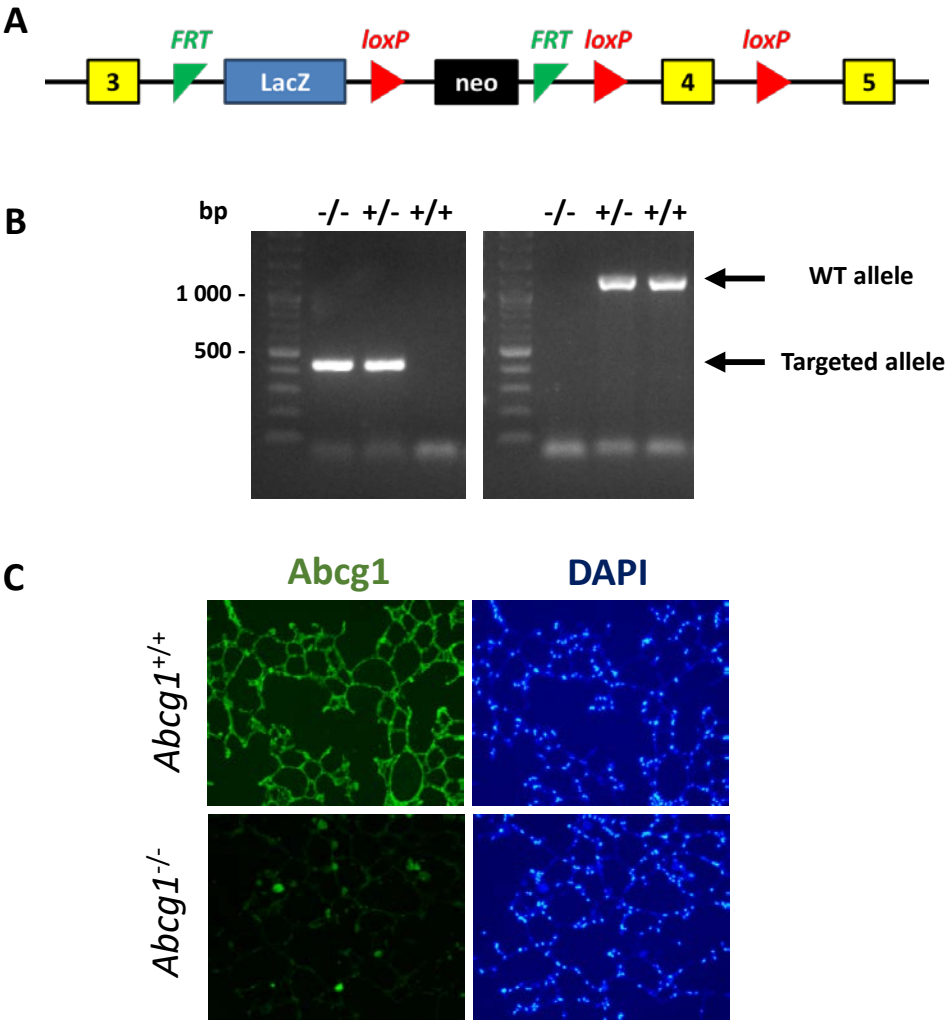

Supplemental Figure 1. Generation of *Abcg1*$^{-/-}$ mice. A, Depiction of the targeted *Abcg1* locus. B, Amplification of genomic DNA with specific primers for the WT or the targeted allele. C, Abcg1 deficiency was confirmed by detection of Abcg1 (green) by immunofluorescence in lung from *Abcg1*$^{+/+}$ or *Abcg1*$^{-/-}$ mice. Nuclei were stained with 4',6'-diamidino-2-phenylindole (blue). Numbered yellow boxes correspond to exons. Neo, neomycin.

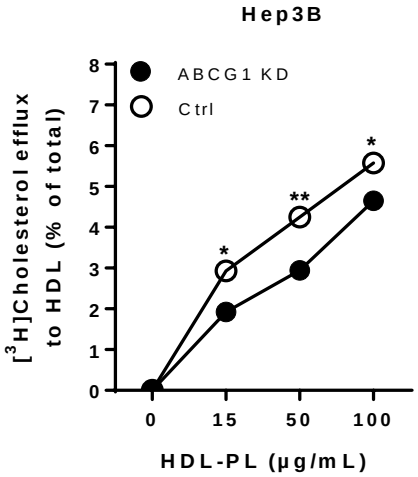

Supplemental Figure 2. **Hepatic ABCG1 expression promoted cholesterol efflux to HDL.** Cellular free [^{3}H]cholesterol efflux to HDL from control (Ctrl) and ABCG1 knockdown (KD) Hep3B cells. Data are means ± SEM, *p<0.05 and **p<0.005 vs controls; PL, phospholipid.

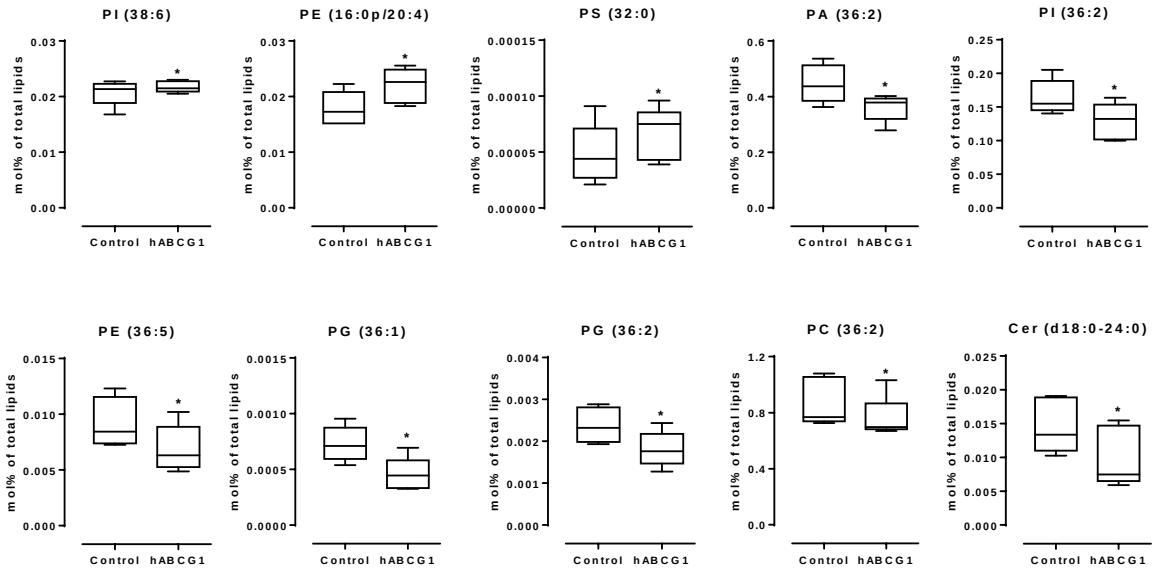

Supplemental Figure 3. **Remodeling of the HDL phospholipidome following the expression of human ABCG1.** Abundance of phospholipid species significantly altered in HDL following the expression of human ABCG1 in female mice (n=16) (*p<0.05 after FDR correction). Cer, ceramide; PA, phosphatidic acid; PC, phosphatidylcholine; PE, phosphatidylethanolamine; PG, phosphatidylglycerol; PI, phosphatidylinositol; pPE, plasmalogen PE; PS, phosphatidylserine.

Supplemental tables.

Supplemental Table 1. Fasting plasma lipid and glucose levels in healthy normolipidemic women according to the rs1378577 SNP.

	ABCG1 rs1378577		
Fasting plasma lipid levels	**All (n=68)**	**T/T (n=40)**	**G/G (n=28)**
TC (mg/dL)	209.8±5.9	212.6±8.0	205.5±8.7
TG (mg/dL)	96.5±5.9	101.8±8.1	88.7±8.6
Glucose (mmol/L)	5.09±0.11	5.11±0.15	5.06±0.16
LDL-C (mg/dL)	130.9±5.7	133.6±8.1	127.0±7.6
HDL-C (mg/dL)	59.5±1.8	58.7±2.4	60.7±2.9
ApoA-I (g/L)	1.55±0.03	1.56±0.04	1.53±0.08
ApoB (g/L)	1.03±0.04	1.04±0.06	1.00±0.07
Lp(a) (mg/dL)	42.7±9.1	39.7±10.1	50.2±21.1

Only subjects carrying either the T/T or the G/G genotype for the rs1378577 (ABCG1 c. -134 T>G) SNP were selected for the study. Subjects were not receiving lipid-lowering therapy. TC: total cholesterol, TG: triglycerides, LDL-C: low density lipoprotein-cholesterol, HDL-C: high density lipoprotein-cholesterol, Apo: apolipoprotein, Lp(a): lipoprotein(a). Values are means±S.E.M.

Supplemental Table 2. Modulation of the HDL lipidome following the expression of human ABCG1.

Lipid species	Control		hABCG1		Remodeling
(normalized to PL)	Mean	S.E.M.	Mean	S.E.M.	
LPC (16:0)	1.13258	0.14522	1.039424	0.10925	
LPC (16:1)	0.01876	0.00193	0.01393	0.00085	
LPC (16:2)	0.00023	0.00005	0.00020	0.00003	
LPC (18:0)	0.79910	0.02638	0.79927	0.07340	
LPC (18:1)	0.20783	0.01526	0.19884	0.00634	
LPC (18:2)	0.26823	0.02098	0.23978	0.01524	
LPC (18:3)	0.00493	0.00045	0.00422	0.00034	
LPC (20:0)	0.00553	0.00076	0.00473	0.00050	
LPC (20:1)	0.00496	0.00062	0.00413	0.00042	
LPC (20:2)	0.00494	0.00072	0.00484	0.00059	
LPC (20:3)	0.02390	0.00274	0.02452	0.00302	
LPC (20:4)	0.07476	0.00992	0.07367	0.00815	
LPC (20:5)	0.00355	0.00055	0.00320	0.00037	
LPC (22:3)	0.00033	0.00005	0.00037	0.00007	
LPC (22:4)	0.00095	0.00009	0.00091	0.00014	
LPC (22:5)	0.00331	0.00048	0.00340	0.00095	
LPC (22:6)	0.03784	0.00295	0.03939	0.00449	
LPE (16:0)	0.01024	0.00097	0.00880	0.00088	
LPE (16:1)	0.00067	0.00009	0.00055	0.00006	
LPE (18:0)	0.01492	0.00096	0.01483	0.00246	
LPE (18:1)	0.01552	0.00416	0.01130	0.00118	
LPE (18:2)	0.01804	0.00220	0.01436	0.00116	
LPE (18:3)	0.00081	0.00018	0.00061	0.00006	
LPE (20:3)	0.00212	0.00035	0.00178	0.00017	
LPE (20:4)	0.02089	0.00215	0.01982	0.00260	
LPE (20:5)	0.00175	0.00023	0.00143	0.00016	
LPE (22:4)	0.00198	0.00032	0.00203	0.00037	
LPE (22:5)	0.00211	0.00035	0.00195	0.00034	
LPE (22:6)	0.02351	0.00341	0.02175	0.00376	
PA (34:1)	0.01210	0.00210	0.01055	0.00175	
PA (34:2)	0.02518	0.00556	0.01857	0.00350	
PA (36:1)	0.00295	0.00019	0.00241	0.00048	
PA (36:2)	0.44617	0.05297	0.36085	0.03280	
PA (36:3)	0.01672	0.00275	0.01207	0.00145	
PA (36:4)	0.02981	0.00275	0.02489	0.00240	
PA (40:5)	0.02238	0.00515	0.02440	0.00338	
PA (40:6)	0.04633	0.00778	0.04309	0.00152	
PC (28:0)	0.00763	0.00190	0.00853	0.00183	
PC (30:1)	0.10952	0.02172	0.08896	0.02086	
PC (30:2)	0.00282	0.00044	0.00264	0.00008	
PC (32:0)	0.17873	0.01214	0.16795	0.03416	
PC (32:1)	0.19680	0.03518	0.14328	0.01442	

PC (34:0)	0.09535	0.02281	0.10738	0.01813
PC (34:1)	1.95468	0.29839	1.70099	0.12852
PC (34:2)	1.09367	0.15859	0.93275	0.08559
PC (34:3)	0.05280	0.00622	0.04227	0.00497
PC (36:1)	0.50193	0.10156	0.47489	0.04000
PC (36:2)	0.87078	0.14706	0.75846	0.10928
PC (36:3)	0.31258	0.04708	0.28571	0.04623
PC (36:4)	1.29392	0.15754	1.38086	0.08645
PC (36:5)	0.12998	0.01430	0.12863	0.01271
PC (36:6)	0.00685	0.00070	0.00619	0.00063
PC (38:2)	0.01570	0.00290	0.01377	0.00180
PC (38:3)	0.11111	0.03152	0.11482	0.02079
PC (38:4)	1.15862	0.13338	1.22160	0.07613
PC (38:5)	0.59352	0.06220	0.58058	0.03315
PC (38:6)	1.41635	0.10816	1.40914	0.10012
PC (40:4)	0.02546	0.00349	0.02472	0.00313
PC (40:5)	0.07976	0.00797	0.07914	0.01464
PC (40:6)	0.48126	0.04946	0.55109	0.02875
PC (40:7)	0.22730	0.02653	0.23347	0.03663
PC (40:8)	0.02743	0.00343	0.02867	0.00457
PE (16:0p/18:2)	0.00527	0.00073	0.00517	0.00069
PE (16:0p/20:1)	0.00039	0.00006	0.00032	0.00007
PE (16:0p/20:2)	0.00014	0.00011	0.00017	0.0007
PE (16:0p/20:3)	0.00083	0.00026	0.00088	0.00019
PE (16:0p/20:4)	0.01785	0.00236	0.02199	0.00252
PE (16:0p/22:4)	0.00280	0.00032	0.00353	0.00071
PE (16:0p/22:5)	0.00243	0.00047	0.00282	0.00066
PE (16:0p/22:6)	0.02169	0.00389	0.02523	0.00259
PE (18:0p/18:1)	0.00406	0.00051	0.00447	0.00025
PE (18:0p/18:2)	0.02155	0.00278	0.01947	0.00189
PE (18:0p/18:3)	0.00348	0.00062	0.00297	0.00019
PE (18:0p/20:3)	0.00196	0.00027	0.00198	0.00045
PE (18:0p/20:4)	0.06057	0.00401	0.05899	0.00464
PE (18:0p/20:5)	0.00784	0.00093	0.00748	0.00052
PE (18:0p/22:6)	0.06069	0.00763	0.05960	0.00387
PE (18:0p/24:5)	0.00299	0.00043	0.00273	0.00021
PE (30:0)	0.00015	0.00004	0.00013	0.00003
PE (32:0)	0.00343	0.00062	0.00374	0.00089
PE (32:1)	0.00214	0.00057	0.00181	0.00048
PE (34:0)	0.00288	0.00032	0.00298	0.00055
PE (34:1)	0.03411	0.01262	0.02882	0.00823
PE (34:2)	0.06372	0.01547	0.04732	0.01126
PE (36:1)	0.00948	0.00269	0.00945	0.00244
PE (36:2)	0.14546	0.04028	0.10814	0.02386
PE (36:3)	0.04865	0.01137	0.036533	0.00958
PE (36:4)	0.07528	0.01115	0.06524	0.01443
PE (36:5)	0.00926	0.00183	0.00691	0.00156
PE (38:2)	0.00751	0.00194	0.00574	0.00096

PE (38:3)	0.01780	0.00299	0.01719	0.00275
PE (38:4)	0.10995	0.00770	0.091336	0.01195
PE (38:5)	0.07441	0.01448	0.06377	0.01291
PE (38:6)	0.10047	0.01466	0.08521	0.01819
PE (40:4)	0.00629	0.00106	0.00577	0.00085
PE (40:5)	0.00811	0.00150	0.00827	0.00120
PE (40:6)	0.02923	0.00411	0.02781	0.00237
PE (40:7)	0.02265	0.00319	0.02122	0.00436
PE (40:8)	0.00778	0.00126	0.00685	0.00046
PG (32:0)	0.00015	0.00003	0.00018	0.00002
PG (34:1)	0.00203	0.00061	0.001413	0.00027
PG (34:2)	0.00137	0.00019	0.00118	0.00019
PG (34:3)	0.00010	0.00001	0.00009	0.00001
PG (36:1)	0.00072	0.00011	0.00045	0.00010
PG (36:2)	0.00238	0.00034	0.00181	0.00029
PG (36:3)	0.00081	0.00016	0.00054	0.00007
PG (36:4)	0.00050	0.00009	0.00044	0.00008
PG (38:2)	0.00001	0.00002	0.00004	0.00002.
PG (38:3)	0.00026	0.00003	0.00024	0.00004
PG (38:4)	0.00062	0.00009	0.00052	0.00006
PG (38:5)	0.00015	0.00003	0.00012	0.00004
PG (38:6)	0.00017	0.00003	0.00016	0.00002
PG (40:6)	0.00015	0.00003	0.00013	0.00004
PG (40:7)	0.00010	0.00004	0.00011	0.00002
PI (32:0)	0.00146	0.00049	0.00115	0.00011
PI (32:1)	0.00224	0.00031	0.00208	0.00031
PI (34:1)	0.01675	0.00215	0.01320	0.00196
PI (34:2)	0.08948	0.01716	0.07949	0.01012
PI (36:1)	0.01467	0.00389	0.01198	0.00181
PI (36:2)	0.16461	0.01935	0.12856	0.02144
PI (36:3)	0.08672	0.00888	0.07295	0.00677
PI (36:4)	0.17447	0.01259	0.17149	0.01154
PI (38:2)	0.01417	0.00312	0.01373	0.00207
PI (38:3)	0.17788	0.03792	0.15424	0.02675
PI (38:4)	1.58835	0.13236	1.67214	0.09920
PI (38:5)	0.13199	0.02231	0.13164	0.01092
PI (38:6)	0.02072	0.00157	0.02176	0.00080
PI (40:4)	0.00615	0.00097	0.00579	0.00086
PI (40:5)	0.01901	0.00247	0.01897	0.00175
PI (40:6)	0.03922	0.00424	0.03844	0.00487
PI (40:7)	0.00484	0.00055	0.00503	0.00105
PS (32:0)	0.00004	0.00001	0.00006	0.00001
PS (32:1)	0.00004	0.00001	0.00005	0.00001
PS (34:0)	0.00003	0.00000	0.00004	0.00000
PS (34:1)	0.00021	0.00008	0.00026	0.00011
PS (34:2)	0.00541	0.00141	0.00548	0.00164
PS (34:3)	0.00097	0.00017	0.00137	0.00021
PS (36:1)	0.00036	0.00023	0.00049	0.00030

PS (36:2)	0.03598	0.01742	0.03711	0.01390
PS (36:3)	0.01348	0.00487	0.01474	0.00365
PS (36:4)	0.02966	0.01016	0.03683	0.01051
PS (38:2)	0.00359	0.00240	0.00301	0.00162
PS (38:3)	0.00896	0.00268	0.01633	0.00782
PS (38:4)	0.13177	0.03807	0.15008	0.04168
PS (38:5)	0.10820	0.05201	0.14565	0.02890
PS (38:6)	0.08966	0.03052	0.10520	0.02021
PS (40:4)	0.00992	0.00458	0.01503	0.00631
PS (40:5)	0.04996	0.01869	0.06033	0.02097
PS (40:6)	0.18103	0.05945	0.22319	0.04760
PS (40:8)	0.12304	0.05512	0.13751	0.03975
Cer (d18:0-24:0)	0.01460	0.00340	0.00996	0.00377
Cer (d18:1-14:0)	0.00009	0.00002	0.00006	0.00009
Cer (d18:1-16:0)	0.00775	0.00019	0.00817	0.00089
Cer (d18:1-18:0)	0.00240	0.00063	0.00285	0.00034
Cer (d18:1-19:0)	0.00015	0.00004	0.00017	0.00001
Cer (d18:1-20:0)	0.00051	0.00006	0.00047	0.00005
Cer (d18:1-22:0)	0.00347	0.00043	0.00297	0.00033
Cer (d18:1-23:0)	0.00327	0.00044	0.00284	0.00047
Cer (d18:1-24:0)	0.00674	0.00083	0.00596	0.00075
Cer (d18:1-24:1)	0.04293	0.00782	0.03691	0.00425
Cer (d18:1-25:0)	0.00155	0.00028	0.00135	0.00026
Cer (d18:1-26:0)	0.00029	0.00011	0.00027	0.00006
Cer (d18:1-26:1)	0.00029	0.00006	0.00025	0.00003
Cer (d18:2-16:0)	0.00019	0.00002	0.00020	0.00002
Cer (d18:2-18:0)	0.00023	0.00005	0.00029	0.00010
Cer (d18:2-20:0)	0.00011	0.00002	0.00010	0.00002
Cer (d18:2-21:0)	0.00003	0.00005	0.00002	0.00001
Cer (d18:2-22:0)	0.00087	0.00012	0.00081	0.00013
Cer (d18:2-23:0)	0.00073	0.00010	0.00060	0.00012
Cer (d18:2-23:1)	0.00005	0.00000	0.00004	0.00000
Cer (d18:2-24:0)	0.00136	0.00024	0.00116	0.00020
Cer (d18:2-24:1)	0.00374	0.00049	0.00317	0.00049
Cer (d18:2-24:2)	0.00018	0.00002	0.00019	0.00004
Cer (d18:2-26:0)	0.00002	0.00001	0.00001	0.00000
Cer (d18:2-26:1)	0.00003	0.00001	0.00002	0.00000
SM (32:1)	0.00999	0.00135	0.01054	0.00146
SM (34:1)	0.47044	0.07312	0.55111	0.12127
SM (34:2)	0.05044	0.00970	0.05456	0.00899
SM (36:1)	0.10010	0.01264	0.11518	0.01121
SM (36:2)	0.03901	0.00870	0.04132	0.00329
SM (38:1)	0.03140	0.00391	0.03561	0.00262
SM (38:2)	0.01495	0.00236	0.01587	0.00155
SM (40:1)	0.09229	0.00783	0.10652	0.00853
SM (40:2)	0.06470	0.00732	0.06651	0.00366
SM (41:1)	0.06231	0.00600	0.06892	0.00532
SM (41:2)	0.05640	0.00381	0.05548	0.00396

SM (42:1)	0.10387	0.04658	0.11362	0.03254	
SM (42:2)	0.62755	0.07133	0.63252	0.05412	
SM (42:3)	0.15810	0.02914	0.22119	0.06145	
SM (42:4)	0.01278	0.00262	0.01475	0.00321	

Lipidomic analysis by LC-ESI/MS/MS of total HDL isolated from *Abcg1*$^{-/-}$ mice following the injection of a control vector (Control) or expressing human ABCG1 (hABCG1). Impact of the hABCG1 expression on the amount of each lipid specie is indicated in green (decrease) or in red (increase). LPC. lysophosphatidylcholine; LPE. lysophosphatidylethanolamine; PA. phosphatidic acid; PC. phosphatidylcholine; PE. phosphatidylethanolamine; PG. phosphatidylglycerol; PI. phosphatidylinositol; PS. phosphatidylserine; Cer. ceramide; SM. sphingomyelin. Values are means±S.E.M (n=18 mice).